Quaternary Science Reviews 67 (2013) 17–38

Contents lists available at SciVerse ScienceDirect

Quaternary Science Reviews

journal homepage: www.elsevier.com/locate/quascirev

High-resolution record of the environmental response to climatic variations during the Last Interglacial–Glacial cycle in Central Europe: the loess-palaeosol sequence of Dolní Věstonice (Czech Republic)

Pierre Antoine [a,*], Denis-Didier Rousseau [b,c], Jean-Philippe Degeai [a], Olivier Moine [a], France Lagroix [d], Sebastian kreutzer [e], Markus Fuchs [e], Christine Hatté [f], Caroline Gauthier [f], Jiri Svoboda [g], Lenka Lisá [h]

[a] Laboratoire de Géographie Physique, Environnements quaternaires et actuels, UMR 8591 CNRS - Université Paris 1 - UPEC, Meudon, France
[b] Laboratoire de Météorologie Dynamique, UMR CNRS-ENS 8539, Paris, France
[c] Lamont-Doherty Earth Observatory of Columbia University, NY, Palisades, USA
[d] Institut de Physique du Globe de Paris, Université Sorbonne Paris Cité, UMR 7154 CNRS, 75005 Paris, France
[e] Department of Geography, Justus-Liebig-University Giessen, 35390 Giessen, Germany
[f] Laboratoire des Sciences du Climat et de l'Environnement, CEA-CNRS-UVSQ, Gif-sur-Yvette, France
[g] Department of Anthropology, Masaryk Univ., Brno, Czech Republic
[h] Institute of Geology, Czech Acad. Sci, Prague, Czech Republic

ARTICLE INFO

Article history:
Received 20 August 2012
Received in revised form
21 December 2012
Accepted 16 January 2013
Available online

Keywords:
Loess palaeosol
Czech Republic
Weichselian
Early-glacial
Grain size
Palaeopedology
OSL
Organic carbon
Environmental magnetism
Malacology

ABSTRACT

High-resolution multidisciplinary investigation of key European loess-palaeosols profiles have demonstrated that loess sequences result from rapid and cyclic aeolian sedimentation which is reflected in variations of loess grain size indexes and correlated with Greenland ice-core dust records. This correlation suggests a global connection between North Atlantic and west-European air masses. Herein, we present a revised stratigraphy and a continuous high-resolution record of grain-size, magnetic susceptibility and organic carbon $\delta^{13}C$ of the famous of Dolní Vestonice (DV) loess sequence in the Moravian region of the Czech Republic. A new set of quartz OSL ages provides a reliable and accurate chronology of the sequence's main pedosedimentary events. The grain size record shows strongly contrasting variations with numerous abrupt coarse-grained events, especially in the upper part of the sequence between ca 20–30 ka. This time period is also characterised by a progressive coarsening of the loess deposits as already observed in other western European sequences. The base of the DV sequence exhibits an exceptionally well-preserved soil complex composed of three chernozem soil horizons and 5 aeolian silt layers (marker silts). This complex is, at present, the most complete record of environmental variations and dust deposition in the European loess belt for the Weichselian Early-glacial period spanning about 110 to 70 ka, allowing correlations with various global palaeoclimatic records. OSL ages combined with sedimentological and palaeopedological observations lead to the conclusion that this soil complex recorded all of the main climatic events expressed in the North GRIP record from Greenland Interstadials (GIS) 25 to 19.

1. Introduction

Over the last decade, much attention has focused on the impact of rapid climate variations, such as Dansgaard–Oeschger (DO) cycles and oceanic cold events (Heinrich events), on European continental environments (Rousseau et al., 2002, 2011; Sánchez Goñi et al., 2002; Sirocko et al., 2005; Müller et al., 2003; Antoine et al., 2009a,b). Located downwind from the North Atlantic Ocean and south of the Fennoscandinavian ice sheet margin, continental Europe, considered as a vast periglacial plain, is well suited for recording the impacts of climate events during the Last Glacial period. Indeed, the European loess belt (Fig. 1) represents the most extensive and continuous continental archive of the Last Glacial and high loess sedimentation rates (Frechen et al., 2003; Fuchs et al., 2007; Antoine et al., 2009a) provide the temporal resolution necessary for recording these millennial scale climate variations.

The pedosedimentary record of loess/palaeosol sequences of the last climatic cycle (Eemian-Weichselian) in Europe is fairly well

* Corresponding author.
E-mail address: pierre.antoine@cnrs-bellevue.fr (P. Antoine).

0277-3791/$ – see front matter © 2013 Elsevier Ltd. All rights reserved.
http://dx.doi.org/10.1016/j.quascirev.2013.01.014

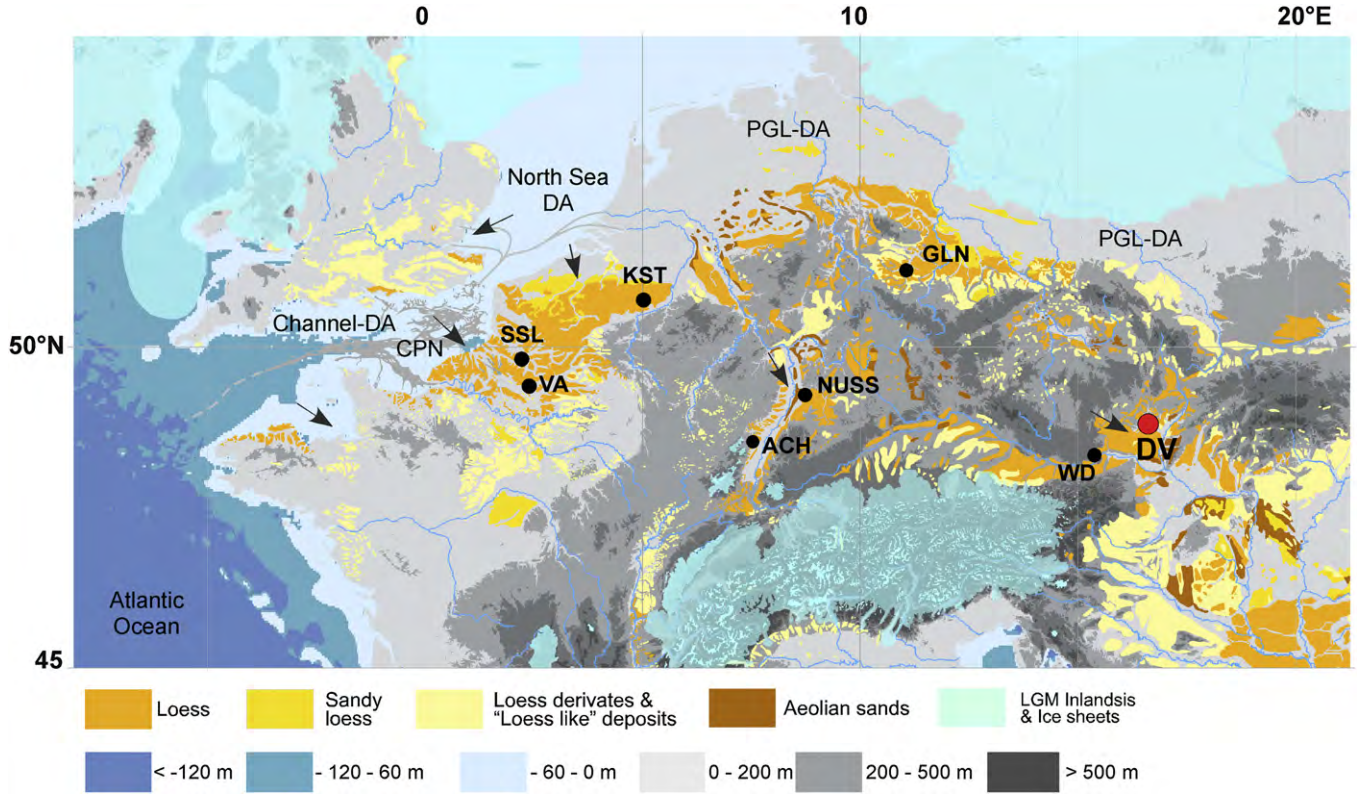

Fig. 1. Location of the Dolní Věstonice site (DV) and of several reference loess sequences on a palaeogeographic map of Europe during the LGM including loess extension and ice sheets. Extension of the continental European loess belt (modified after Haase et al., 2007; GIS data kindly provided by D. Haase), loess from southern England according to Catt (1985, 1988), loess from Paris basin according to Antoine et al. (1999b). Arrows: reconstructed general prevailing directions of palaeowinds (according to loess distribution, morphology and heavy minerals: Antoine et al., 2009a,b; Lautridou, 1987). Extension of the Fennoscandian ice sheet during the LGM (according to Ehlers et al., 2011; GIS data kindly provided by J. Ehlers). Abbreviations: CPN: Channel palaeoriver network (according to Auffret et al., 1982), North Sea DA and Channel DA: North Sea and Channel deflation areas during periods of low sea level (−120 m), PGL DA: proglacial deflation area south of the Fennoscandian ice sheet. SSL: Saint-Sauflieu (France), VA: Villiers-Adam (France), NUSS: Nussloch (Germany); KST: Kesselt (Belgium); ACH: Achenheim (France), GLN: Gleina (Germany), WD: Willendorf (Austria), DV: Dolní Věstonice.

constrained through stratigraphical, palaeopedological and geochronological (luminescence and ^{14}C) investigations over the last thirty years (Sommé et al., 1980, 1986; Haesaerts et al., 1981, 1999, 2003; Lautridou et al., 1985; Zöller et al., 1988; Zöller and Wagner, 1990; Juvigné et al., 1996; Rousseau et al., 1998a,b; Antoine et al., 1999a, 2001, 2003a,b; Frechen, 1999; Meijs, 2002; Meszner et al., 2011). More recently, investigations have focused on producing high-resolution multi-proxy records using pedostratigraphy, grain size analysis, organic carbon geochemistry and malacology (Hatté et al., 1999, 2001a; Antoine et al., 2001, 2002; Moine et al., 2002, 2008; Haesaerts et al., 2003). These efforts are concomitant with important developments in luminescence and organic ^{14}C age determination methods improving the geochronology of the last climatic cycle (Hatté et al., 1998, 2001b; Frechen et al., 2001, 2003; Lang et al., 2003; Fuchs et al., 2007; Tissoux et al., 2009; Frechen and Schirmer, 2011; Stevens et al., 2011; Terhorst et al., 2011; Fuchs et al., 2012; Kreutzer et al., 2012).

One example of such efforts is the work done on the Nussloch loess/palaeosol sequence (Germany), a key reference record demonstrating that loess deposition can be cyclic and extremely rapid (≥1 mm/a, Antoine et al., 2009a; Rousseau et al., 2002, 2007). Here, variations in a grain-size ratio recovered a cyclic pattern alternating between fine grained tundra gley layers (G) and coarse grained Loess Events (LE) over the ca 34–17 ka period (Antoine et al., 2009a). A correlation between grain size variations and dust content in the Greenland ice-core record was demonstrated, suggesting a connection between North Atlantic high latitudes and West-European atmospheric circulations (Rousseau et al., 2002, 2007; Antoine et al., 2009a) and encouraging attempts to model the provenance of aeolian dust and direction of transport during the Upper Pleniglacial (Antoine et al., 2009a; Sima et al., 2009).

In eastern Europe, the pattern of loess/palaeosol sequences in Ukraine and Serbia are also influenced by North Atlantic climate events (Fuchs et al., 2007; Antoine et al., 2009a,b; Rousseau et al., 2011). The present study aimed to obtain a high-resolution multiproxy record of the Dolní Věstonice loess/palaeosol sequence in the Czech Republic in order to bridge the gap in observations along a ~49°N latitude band between Germany and Ukraine. This location was also motivated by (1) the wealth of previously published data identifying this site as one of the thickest, most contrasted and well preserved record of the last climatic cycle in Europe and especially of the Early-glacial period (MIS 5d-a and early MIS 4), (2) the occurrence, in the immediate surroundings, of well-dated Upper Palaeolithic archeological sites and ^{14}C ages for the base of the Upper Pleniglacial (UPG) and (3) the accessibility to the sequence.

2. Site description, previous work and open chronological questions

Dolní Věstonice (DV) is located in Moravia, the southeastern region of the Czech Republic, and in the central part of the European loess belt (Fig.1). During the Last Glacial, the site was surrounded by the Alpine ice cap to the South (~100 km) and the Fennoscandinavian ice sheet to the North (Ehlers et al., 2011) (~300 km). The DV loess-palaeosols sequence (48°53′11.5″ N, 16°39′16″ E, 165 m a.s.l.) is located north of the Pavlov Mountain, which culminates at 549 m a.s.l. some 2 km south of the site, and on the southern shoreline of the Dyje River flood plain. The Dyje River

is a sub-tributary of the Danube River and, in the vicinity of Dolní Věstonice, river engineering work from 1975 to 1988 transformed the flood plain into a water reservoir. The DV section is exposed in a former brickyard along a vertical profile created during an archaeological excavation led by Klíma in the 1960's.

The climate of the Czech Republic, and of Moravia in particular, is continental and characterised by very cold winters and warm and humid summers, as shown by the 1971–2000 climate data for Retz/Windmuehle (Austria): annual precipitation: 492.34 mm, mean annual temperature: +9.64 °C; average low temperature of the 6 coldest months (ONDJFM): +3.14 °C/3 coldest (DJF): −0.06 °C; average high temperature of the 6 warmest months (AMJJAS): 16.09 °C/3 warmest (JJA): 18.98 °C (Klein Tank et al., 2002).

The pioneering archeological work at DV was lead by Absolon et al. (1933), Absolon (1938a,b), Bohmers (1941) and Lais (1954) and later coordinated with stratigraphy, palaeopedology and malacology investigations (Ložek, 1953; Klima et al., 1962; Ložek in Klima et al., 1962; Demek and Kukla, 1969; Kukla, 1975). Kukla (1977), based in part on observations made along the DV sequence, defined a stratigraphic model of loess deposition over the last climatic cycle. The model proposed that a complete cycle record is composed of a loess horizon, a pedocomplex (PK I, PK II and PK III) of a given soil type, a thin aeolian silt horizon (Markers) and a Lehmbröckelsand horizon (pellet sands).

More recently, the geochronology of the DV sequence has been analysed by means of luminescence, radiocarbon and amino acid racemisation of molluscs' shells (Musson and Wintle, 1994; Zöller et al., 1994; Forster et al., 1996; Damblon and Haesaerts, 1997; Frechen et al., 1999). Despite these numerous studies, the chronostratigraphic interpretation remains open, especially for the basal soil complex between about 13.50 m and 9.50 m (Fig. 2) (Musson and Wintle, 1994; Zöller et al., 1994; Oches and McCoy, 1995; Frechen et al., 1999).

For example, Kukla (1961) and Demek and Kukla (1969) assumed a paedological continuity between the Bt horizon (unit 21a, this study) and the humic soil horizon (unit 19) leading them to its labelling as a single pedocomplex (PK III in Fig. 2). The validity of this assumption has been questioned by Frechen et al. (1999) who observed scattered carbonate nodules across both of these horizons suggesting an erosional discontinuity which invalidates the continuous pedocomplex hypothesis for PK III. Moreover, the presence of steppe malacofauna fragments (especially *Helix pomatia*) within the lower half of the humic horizon (unit 19) and the overlying aeolian silt (unit 18) observed by Klima et al. (1962), lead them to propose that locally the interglacial soil horizon was reworked and partly eroded prior to the formation of unit 19 chernozem soil. Based on TL and IRSL age determinations, Musson and Wintle (1994) also proposed a partitioning of PK III allocating the chernozem palaeosol of unit 19 to marine isotopic stage (MIS) 5c and the Bt horizon of unit 21a to MIS 5e.

Inconsistencies in the chronostratigraphic interpretation and age determinations of PK II soil complex (Fig. 2, units 11–15) lead to another open question. In Kukla (1975), chernozem soils of units 11 and 15 are proposed to represent MIS 5a and 5c respectively, based on a correlation of the magnetic susceptibility record with global marine $\delta^{18}O$ records. However, TL and IRSL ages obtained on these two chernozem soils are markedly younger suggesting a development of unit 15 during MIS 5a and of unit 11 at an even younger Early-glacial time (Musson and Wintle, 1994) or even contemporaneously with MIS 3 (Frechen et al., 1999).

These chronostratigraphic issues are of the utmost importance. Mutli-proxy studies are likely to provide the necessary constraints needed to further our understanding of these open questions. To our knowledge, the DV loess and palaeosol sequence has previously been investigated in only three palaeoenvironmental and palaeoclimate motivated studies. Oches and Banerjee (1996) presented the variation of several rock magnetic parameters characterizing the magnetic granulometry. Shi et al. (2003) presented bulk sediment grain-size, organic matter content and magnetic susceptibility data and their correlations with North Atlantic climate proxies derived from Greenland ice cores and marine sediment core V28-31 as evidence of millennial scale climate events being recorded in central European loess. Their geochronological constraint, based on one ^{14}C age, remains very weak. Lastly, Bábek et al. (2011) combined diffuse reflectance spectroscopy and bulk magnetic susceptibility to infer the degree of pedogenic weathering and test whether a universal model of pedogenic weathering was applicable.

Since the detailed stratigraphy of the DV sequence by Klima et al. (1962), subsequent studies have progressively over-simplified the pedo-sedimentary description of the site's stratigraphy. These over-simplifications render correlations of sample location between records difficult. For the above reason a detailed stratigraphic description based on both field and thin section observations complemented by laboratory analyses of grain size, organic carbon and $CaCO_3$ are presented in this study. The goals are to (1) re-define the pedostratigraphy of the DV sequence, a reference site, in light of new data presented herein, of recently obtained high resolution luminescence ages (Fuchs et al., 2012) and of the knowledge acquired since the pioneering work of the 1960's and 1970's, and (2) provide a robust interpretation of palaeoenvironmental changes enabled by the new record sampled and analysed continuously and at a high resolution.

3. Methods and analyses

3.1. Field work (stratigraphy and sampling)

A 15 m high wall of the DV brickyard was scraped using cliff-hanging equipment removing approximately 0.5–1 m thick layer of dried loess penetrated by desiccation cracks and revealing a fresh pristine surface. The stratigraphy based on field observations was described and drawn at a 1:20 scale (Fig. 2, Table i – Supplementary Material). The DV09 loess/palaeosol record was recovered following the Continuous Column Sampling (CCS) protocol described in Antoine et al. (2009a). Bulk material was sampled at a 5 cm depth resolution yielding 300 bulk samples of approximately 300–400 g each (Fig. 2B and G). They were homogenized in the field and sub-sampled twice. One sub-sample is for carbon isotope geochemistry and was dried at low temperature as soon as possible to ensure safe storage as recommended by Gauthier and Hatté (2008), the second is for rock magnetic analyses and the remaining material for grain-size distribution analyses. A larger volume (~10 L) bulk sampling was conducted over the 5.50–6.40 m depth interval at a 10 cm depth resolution yielding 9 samples. The content of the ~10 L bags were wet sieved in the field along the Dyje River using a 420 μm mesh. The sieved material was brought back to the laboratory for mollusc shell identification and population counting. Undisturbed block-samples (~15 × 8 × 5 cm, $n = 14$) were extracted from the profile and from which thin sections were prepared in the laboratory and analysed under an optical microscope providing complementary, finer scale, observations (Fig. 3). Fragments of charcoal were sampled at about 6.10 m depth for radiocarbon dating. Lastly, fifteen samples for OSL dating (Fuchs et al., 2012) were sampled during the night (Fig. 2, BT-752 to BT-766).

3.2. Grain size analysis

Grain size distributions were measured using the Fluid Module of a Beckman Coulter LS-230 Laser Particle Size analyser. For each

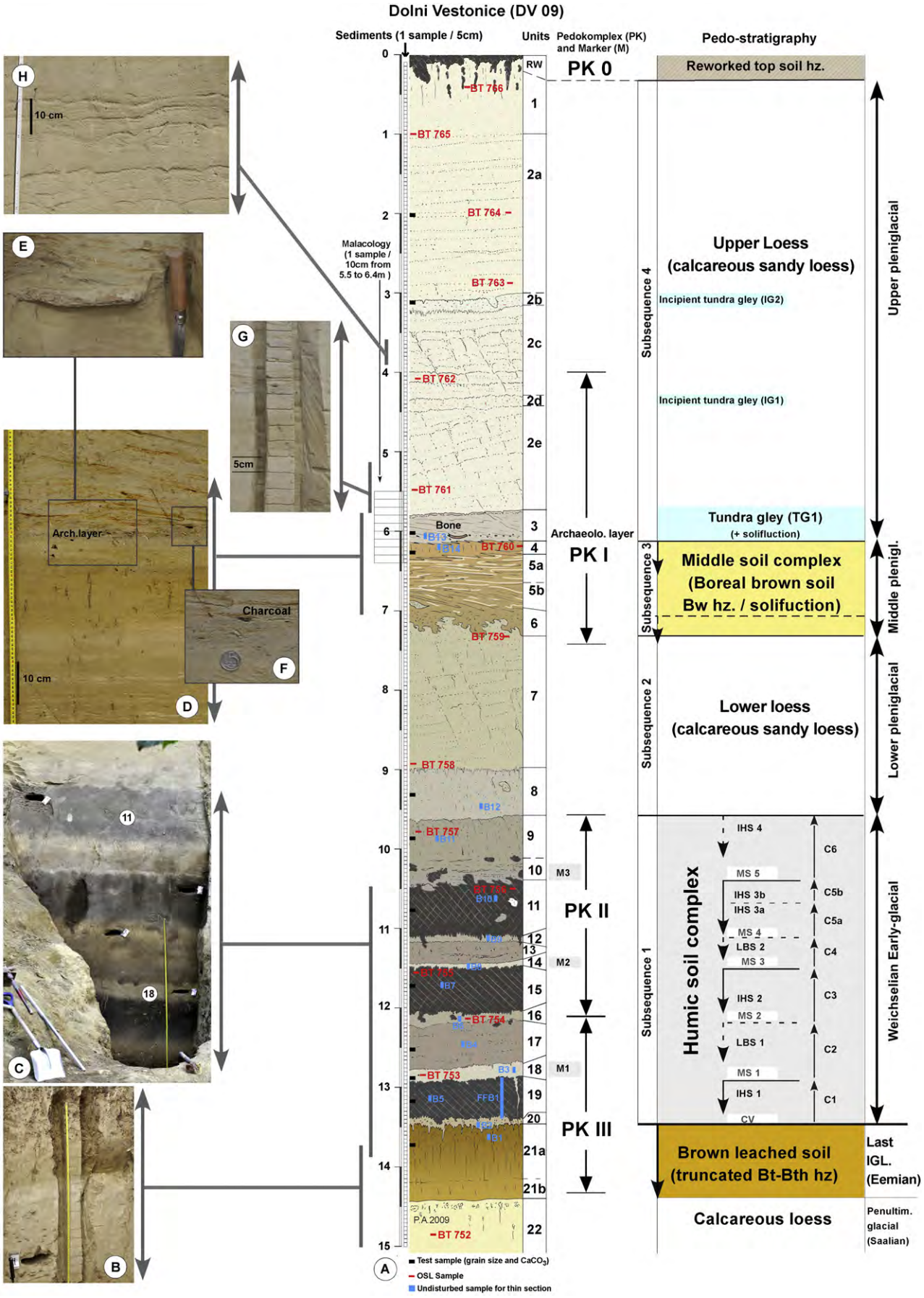

Fig. 2. Dolní-Vestonice profile P1 2009: stratigraphy, sampling strategy, location of samples, correlation with Kukla's stratigraphic scheme and chronoclimatic interpretation. CV: colluvium, IHS: isohumic soil horizons (chernozems), LBS: ("Lehmbröckelsands"), MS: marker silts, C1 to C6: pedosedimentary cycles.

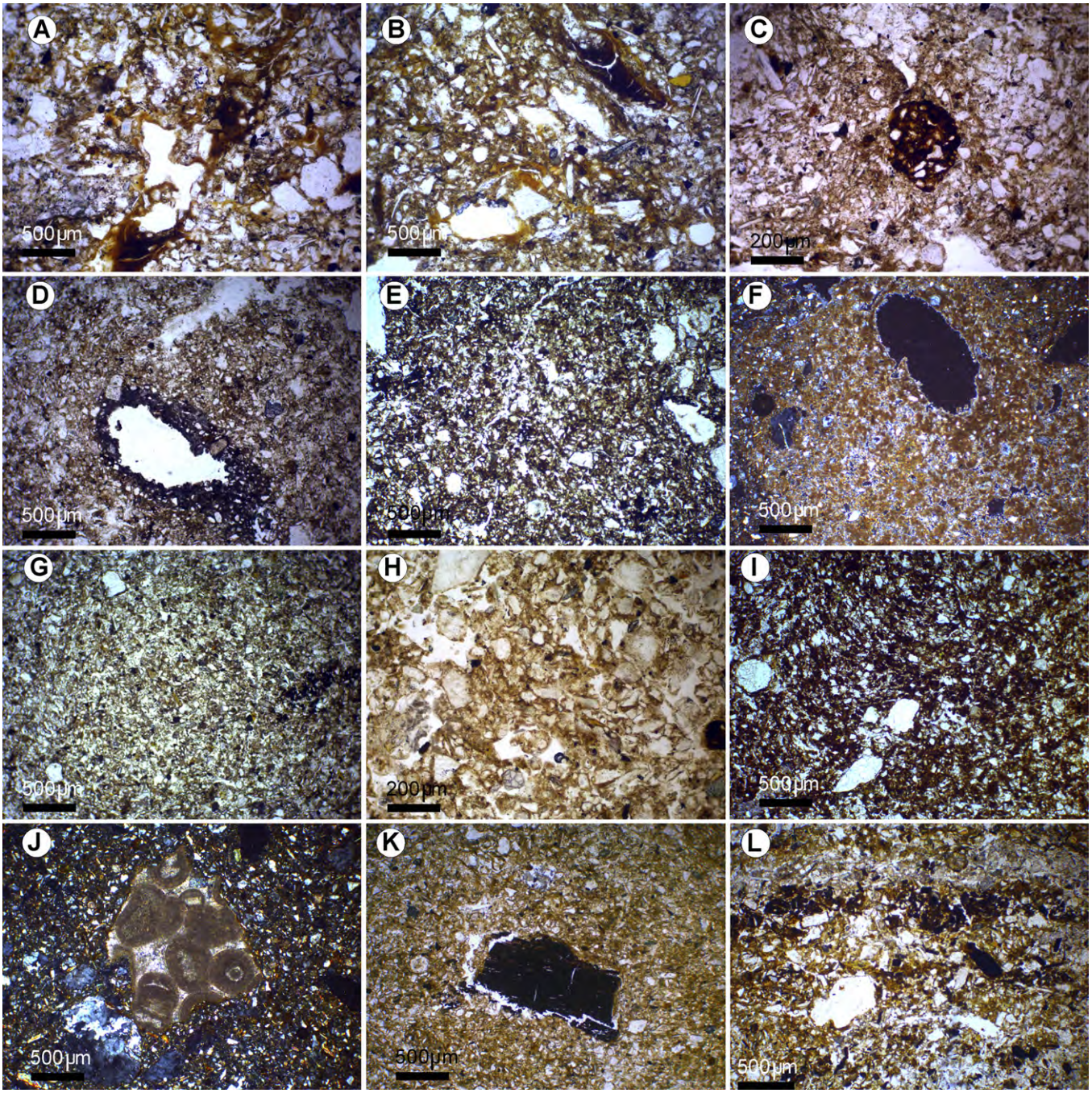

Fig. 3. Thin sections (location of samples: see Fig. 2). A & B – Unit 21a: clay coatings: yellow then dark brown stratified humic clay coatings. C – Unit 20 (CV): reworked Fe–Mn hard nodules and soil papules from 21a. D – Unit 20 (CV): $CaCO_3$ precipitation around a biopore (hypocoating). E – Unit 19 (IHS 1): clayey organic matrix. F – Unit 19 (IHS 1): calcareous nodule. G – Unit 18 (MS1): homogeneous silty texture. H – Unit 17 (LBS 1): impregnation of the matrix by clay coatings. I – Unit 11 (IHS 3): clayey humic matrix. J – Unit 12 (MS 4): occurrence of a carbonate grain from oolithic limestone. K – Unit 4 (brown soil Hz): micro-charcoals spread in the matrix of the brown soil horizon. L – Unit 3 (TG 1): deformed laminations underlined by iron oxide bands and reworked charcoals (archaeological layer). (For interpretation of the references to colour in this figure legend, the reader is referred to the web version of this article.)

sample, 10 g of sediment was dispersed in 400 mL solution concentrated with 0.5% sodium hexametaphosphate in deionised water. Dispersion was improved by agitating the solution in a rotating shaker for two hours. Subsequently, the solution was wet sieved with a 160 µm mesh. The coarse fraction ($d > 160$ µm) was dried at 45 °C and its dry weight was recorded. Deionised water was added to the remaining solution achieving a total volume of 600 mL. A propeller stirrer maintained the solution well homogenized while 2–4 mL aliquots were sub-sampled with a graduated transfer pipette for grains size analyses. The sample preparation protocol was validated by obtained reproducible results from multiple aliquots for 10 different sampling depths. Instrumental drift of the particle size analyser was assessed by analysing a control sample prior to each measurement series.

Particle size distributions determined on a single sample using the classic "sieving and pipette" method or by laser diffraction will differ due to analytical limitations intrinsic to each method. The assumption of spherical particles and the use of a uniformed

refractive index are two examples of analytical limitations (Konert and Vandenberghe, 1997; Buurman et al., 2001). An inter-method calibration was achieved for the DV loess and palaeosol sequence using 12 bulk samples (Table ii – Supplementary Material, see Fig. 2 for test sample location). For DV09, the classical grain size limits following the sieving and pipette method at 2 μm for clay, at 20 μm for fine silt and at 50 μm for coarse silt correspond to 6, 20 and 61 μm, respectively, for the laser diffraction grain size analyser used in this study. The calibration is in agreement with observations published by Konert and Vandenberghe (1997) and Ramaswany and Rao (2006).

3.3. Bulk magnetic susceptibility

Magnetic susceptibility was measured both in the field and in the laboratory. Field measurements were conducted with a Bartington MS2F probe, operating at 580 Hz, at a 10 cm depth interval recording 10 measurements, equally spaced across approximately a width of one metre, at each stratigraphic sampling depth. A higher resolution record of low-field mass specific magnetic susceptibility (χ) was obtained from the continuous bulk sample. The laboratory measurements were conducted on subsamples weighing between 314 mg and 441 mg (375 ± 27 mg) using a KLY-3 susceptibility metre operating with magnetic field amplitude of 300 A/m and a frequency of 875 Hz.

3.4. Carbon isotope geochemistry

The bulk material was sieved using a 250 μm mesh in order to remove coarse sands, molluscs shell fragments or calcified roots and then homogenized. At room temperature, in pre-combusted glass beakers, the fraction finer than 250 μm was soft leached in HCl 0.6 N ultra-pure water solution and dried at 50 °C. This process removes all carbonate. Samples were then crushed in pre-combusted glass mortar and homogenized prior to carbon content and $\delta^{13}C$ analysis. Handling and chemical procedures are consistent with the necessary precautions to be applied with low carbon content sediment.

Organic carbon and carbonate content was measured on every sediment sample. Total carbon was analysed on the bulk sediment while organic carbon was analysed on the finer than 250 μm fraction leached sediment. About 15–20 mg of sediment was weighed in tin cups for measurement (with a precision of 1 μg). The sample was combusted in a Fisons Instrument NA 1500 Element Analyzer and carbon content determined with the Eager software. A standard was inserted every 10 samples. Inorganic carbon content in bulk sediment was calculated assuming that mineral carbon exists only as $CaCO_3$. Results are reported in % weight of carbonate/bulk sediment and in %weight organic carbon/bulk sediment.

Carbon isotope analyses were performed online with a continuous flow EA–IRMS coupling: Fisons Instrument NA 1500 Element Analyzer coupled to a ThermoFinigan Delta + XP Isotope-Ratio Mass Spectrometer. Two home internal standards (oxalic acid, $\delta^{13}C = -19.31\%$ and GCL, $\delta^{13}C = -26.70\%$) were inserted every five samples. Each home standard was regularly checked against international standard. Results are reported in the δ notation:

$$\delta^{13}C = (R_{sample}/R_{standard} - 1)*1000$$

where R_{sample} and $R_{standard}$ are the $^{13}C/^{12}C$ ratios of the sample and the international standard VPDB, respectively. Three measurements were acquired to ensure reproducibility. The external reproducibility of the analysis is better than 0.1%, typically 0.06%. Extreme values were re-checked.

3.5. ^{14}C dating

Charcoals fragments from the Gravettian layer were sampled at the base of unit 3 (6.10 m depth) for radiocarbon dating. The 6.10–6.15 m layer sieving yielded millimetre size charcoal fragments and a large shell of mollusc that both were ^{14}C dated.

Charcoal fragments were treated according to the classical AAA protocol to remove humic and fulvic acids from the charcoal with HCl 1 N, NaOH 0.1 M, ultrapure water and hot rinsing (Hatté et al., 2001c). Both AAA resistant residue and humic acid were combusted under pure O_2 flow in a line designed for very small samples. Pure O_2 is preferred to the classical CuO as purity and C-free is easier to check on gas than on porous material.

The mollusc shell was mechanically cleaned in an ultrasonic bath using ultrapure water. HNO_3 1% was then used to remove superficial carbonate and oxidize superficial organic matter that might result from subsequent contaminating processes. Carbonate is then hydrolysed by H_3PO_4 into CO_2 on semi-automated line (Tisnérat-Laborde et al., 2001).

Evolved CO_2 was then dried, purified, measured and sent to the French national structure for physical measurement (LMC14). ^{14}C age is evaluated by comparison with international and home standards. Calibrated ages are obtained from Calib6.0 (Reimer et al., 2009).

3.6. Terrestrial mollusc

The column of molluscan samples encompasses the Middle-Upper Weichselian transition (units 2e to 5a, Fig. 2) and crosses the archaeological layer and the tundra gley horizon, rich in molluscs, allowing us to depict the associated environmental dynamics. In the laboratory, we hand-picked under a binocular all entire shells and unique shell fragments (apices, apertures), and also whorl fragments of taxa that were not represented by previous categories of elements. All shells and fragments have been identified and counted according to Ložek (1964) (Table iii – Supplementary Material).

Concerning the rest of the sequence that has not been sampled in 2009, former malacological data published by Ložek in Klima et al. (1962) (Table iv – Supplementary Material) are referred to in the discussion (Part 5) with respect to some environmental put forth. In addition, according to Ložek, malacofauna from the basal humic soil complex (PK II and upper PK III) are species-limited (only 3 to 9 species per sample) and rather poor in individuals (<65 shells per sample) despite a volume of 40 L per sample. Moreover, because undetermined *Helicacea* fragments are present in most of his samples from the basal humic soil complex, they have no particular value in discriminating environmental conditions of the units within the complex, and thus, have not been taken into account in our discussion (Part 5).

4. Results

4.1. Stratigraphy

The DV 09 profile is composed of a complex succession of 22 pedosedimentary units (28 if including sub-units). Facies interpretation of the pedosedimentary units are presented in Table i – Supplementary Material, and are based on field observations (Fig. 2), thin section observations (Fig. 3) and sedimentological analyses of grain size, organic carbon and $CaCO_3$ percentages. Four sub-sequences (I–IV) have been distinguished from the top of the Last Interglacial Bt horizon (unit 21) to the surface of the upper loess (unit 1):

Subsequence I: Basal humic soil complex (BHSC: unit 20 to 9)
Subsequence II: Lower sandy loess (unit 8 & 7)
Subsequence III: Middle brown soil complex (unit 6 to 4)
Subsequence IV: Upper sandy loess including tundra gley layers (unit 3 to 1).

4.2. Grain size analysis

4.2.1. Facies differentiation

The DV grain size data ($N = 300$) are plotted in Fig. 4 using a ternary diagram. The end-members used to construct the ternary diagram are the three main grain size classes defined as: fine sands (61–160 μm), coarse silts (20–61 μm), and fine silts and clays (≤20 μm). The cumulative percentage of these three variables range from 27 to 66% for the clays and fine silts, from 24 to 41% for the coarse silts, and from 10 to 45% for fine sands. Spatially, the data set defines a crescent-moon shape distribution with at its apexes a "loess pole" and a "soil pole". Data lying between these poles correspond to weakly weathered loess and marker silts.

The "soil pole", composed of palaeosol samples, is characterised by ~10–17% fine sands, ~25–35% coarse silts, and 50–65% particles finer than <20 μm. The upper part of the "soil pole" is occupied by the horizons in which the pedogenesis is the most advanced. Following this logic, the isohumic soil of unit 15 (IHS 2) which shows by far the highest clay content is also the more pedogenically developed soil, followed by the Lehmbröchelsand of unit 17 (LBS 1), the interglacial soil of unit 21a (Bth) (21a), the boreal brown soil of units 4and 5a (BBS), IHS 1 (unit 19), LBS 2 (unit 13) and finally IHS 3b and 3a (unit 11).

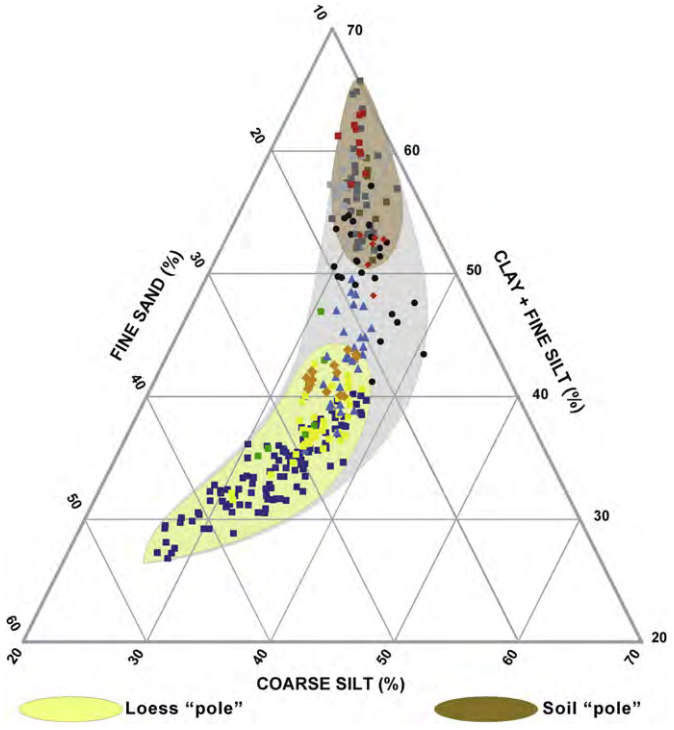

Fig. 4. Ternary diagram of the main grain-size classes of the loess and paleosols from the Dolní Věstonice sequence (300 samples). Blue squares: Upper Pleniglacial loess (Units 1 to 2e); Yellow squares: Lower Pleniglacial loess (Units 7 & 8); Orange diamonds: Saalian loess (Unit 22); Blue triangles: weakly weathered loess (Units 9,5b, 6); Green squares: Tundra gley (Unit 3); Black circles: Marker silts (Units 18, 16, 14, 12, 10); Brown squares: Brown soil horizons (Units 5a, 4); Deep grey squares: IHS, Isohumic soils (Chernozem, Units 11, 15, 19); Light grey squares: LBS horizons (upbuilding humic horizons/colluvial deposits, Units 13, 17); Red diamonds: Interglacial Bt (Unit 21b); Red squares: Interglacial soil (Unit 21a, Bt-Bth).

The boreal brown soil horizons (units 4 and 5a) are characterised by less clay and fine silt percentages than the basal soil complex (Unit 21 to 9). IHS 1, 2, 3a and 3b are more scattered within the range of the "soil pole" while the LBS 1 and 2 horizons are more tightly grouped along the sandier facies of the range. Finally, units 21a and 21b of the interglacial brown leached soil (Bt – Bth) are clearly different where by the upper unit 21a has a higher amount of clay and fine silt and a weaker amount of coarse silt than unit 21b indicative of a higher degree of pedogenesis..

The "loess pole" is characterised by ~20–45% fine sands, ~25–40% coarse silts and ~25–45% particles finer than <20 μm. The amount of fine sands present in the DV loess exceeds what is expected for typical loess (~15%). It would therefore be more accurate to characterise DV loess as sandy loess to silty sands. The Saalian loess of unit 22 has lower sand content (~20–25%) than Weichselian Lower Pleniglacial loess of unit 8 and 7 (~25–35%) and Upper Pleniglacial loess of units 2 and 1 (~25–45%). The tundra gley horizon of unit 3 (TG1) most resembles Lower Pleniglacial loess.

In the zone between the two poles are samples from weathered units 5b and 6 and incipient isohumic humic soil IHS4 (unit 9) and the best preserved marker silts (units 18 & 16). Compared to the loess these marker silts show enrichment in fine particles (clay and fine silt) and a markedly lower fine sand content.

Other grain size indexes such as the U-ratio (Vandenberghe et al., 1998), or the Grain Size Index (GSI) (Antoine et al., 2002, 2009a) are considered to be good proxies of wind strength associated to loess deposition (Vandenberghe and Nugteren, 2001; Nugteren et al., 2004; Pendea et al., 2009). The latter is shown in Fig. 5. The GSI increases throughout the Lower Pleniglacial loess units 8 and 7 and the Upper Pleniglacial loess unit 2 before dropping through the most recent loess unit 1.

4.2.2. Main features of the record

The continuous records of the sequence's grain size variation show a very good correlation with field observed stratigraphic boundaries (Fig. 5).

For example, clay % is very contrasted between loess horizons and units of the basal soil complex (units 9–21) and with the Middle Pleniglacial soil complex (units 6 to 4). Clay % is less than 15% in loess horizons and above 20% in the soil complexes where maximum values of 34% clay are reached in IHS 2 (unit 15). The thin (4–10 cm) marker silt (MS) units 12, 14, 16 and 18 represent 20–22% clay content troughs in the record of the BHSC. Within the Middle Pleniglacial soil complex, units 4 and 5a present clay content enrichment while units 5b and 6 portray loess like clay content %.

The good correlation between peaks in clay content, peaks in magnetic susceptibility and peaks in organic carbon % records (Figs. 5 and 6) reinforces the pedological origin of the clay enrichment. The relationship between enhanced magnetic susceptibility values and humic soil development can be related to *in situ* production of ultrafine iron oxide grains (~30 nm) during pedogenesis (Maher and Taylor, 1988; Maher, 2011). A correlation between clayey humic soil horizons and magnetic susceptibility peak values is systematically observed in the Weichselian Early-glacial soil complexes from Western Europe (Antoine et al., 1999a, 2003a,b).

While both Pleniglacial loess intervals show very poor (12–15%) clay content with no significant variations as generally observed in other allochthonous European loess (Vandenberghe et al., 1998; Antoine et al., 2009a), the fine sand fraction (61–160 μm) exhibits well marked abrupt coarse-grained events (Fig. 5). These are especially well expressed in the upper part of the sequence within loess unit 2. We also observe a progressive coarsening of the loess deposits during this period, followed by a sharp decrease in coarse particle percentages at the boundary between units 1 and 2a best observed in the GSI record.

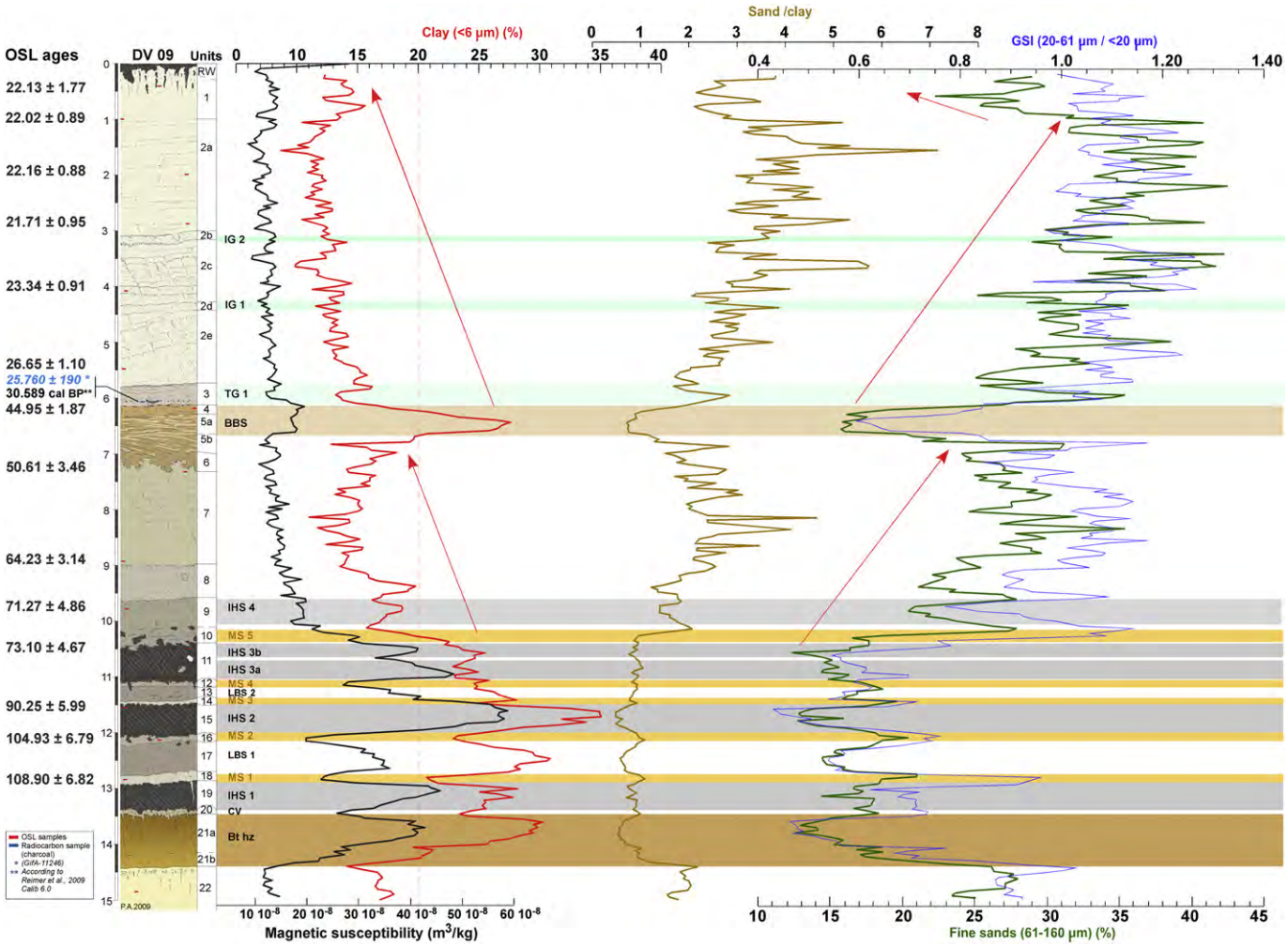

Fig. 5. DV 09: magnetic susceptibility (χ), clay and fine sand percentages, sand/clay ratio, grain size index, OSL (quartz) & ^{14}C (charcoal) dates (^{14}C was performed on the AAA-resistant residue (Hatté et al., 2001b) and the humic acid fraction).

The GSI and fine sand % content records co-vary throughout the BHSC, the brown soils of units 4 and 5a and in the tundra gley of unit 3 (Fig. 5). This is not the case through the sandy loess of units 2 and 1 where peaks in the GSI record correspond to troughs in the fine sands % record. The discordance originates from the importance of the fine sand % in DV loess in the upper 6 m (average 33%), a grain size fraction not taken into account in the GSI. The record of the ratio of fine sand % to clays co-varies with the GSI throughout unit 2 (Fig. 5).

Finally, the main features of the grain size record (as for magnetic susceptibility or organic carbon) are closed to those evidenced by Shi et al. (2003). For example, several major variations appear in both records especially at the boundary between Upper loess deposits and the brown soil of unit 4 (−6.2 m) and at the top of IHS 3b (at ~10.4 m). Nevertheless, a detailed correlation of both records, and especially of the various coarse grain peaks within the sandy loess units, appears not possible, likely owing to the oversimplified stratigraphy of Shi et al. (2003) and differences in sampling strategy and analytical procedures.

4.3. Radiocarbon dating

Two ^{14}C activity measurements were performed on a charcoal extracted from the archaeological layer (base of unit 3, Fig. 2): AAA resistant residue yields for 25 760 ± 190 yrs BP and the humic acid fraction for 24 460 ± 140 yrs BP. The younger age obtained for the humic fraction indicates that post-fossilization organic carbon was effectively removed from the sample and concentrated in the humic fraction. The only slight shift between both ages indicates that the post-fossilization contamination was introduced only slightly after the charcoal fossilization and would not induce a large error if not totally removed.

The data provide a clear and reliable uncalibrated age of the charcoal at 25 760 ± 190 yrs BP (cal BP 30 255—cal BP 30 982). Likewise age obtained on mollusc shells clearly agrees with charcoal result by yielding for 25 870 ± 160 yrs BP (cal BP 30 341—cal BP 31 003). Combination of charcoal and shell ages provides an unambiguous uncalibrated age of 25 820 ± 190 yrs BP to the archaeological layer at the base of TG1 (unit 3).

4.4. Magnetic susceptibility

Field and laboratory measurements of bulk magnetic susceptibility reveal similar variations where the latter provides a higher resolution and a more quantitative measure of the mass specific bulk magnetic susceptibility (χ) of individual sampling interval (Fig. 5).

Loess of subsequence IV (units 3–1, $n = 123$), sub-sequence II (units 8–7, $n = 44$) and below subsequence I, presumably of Saalian

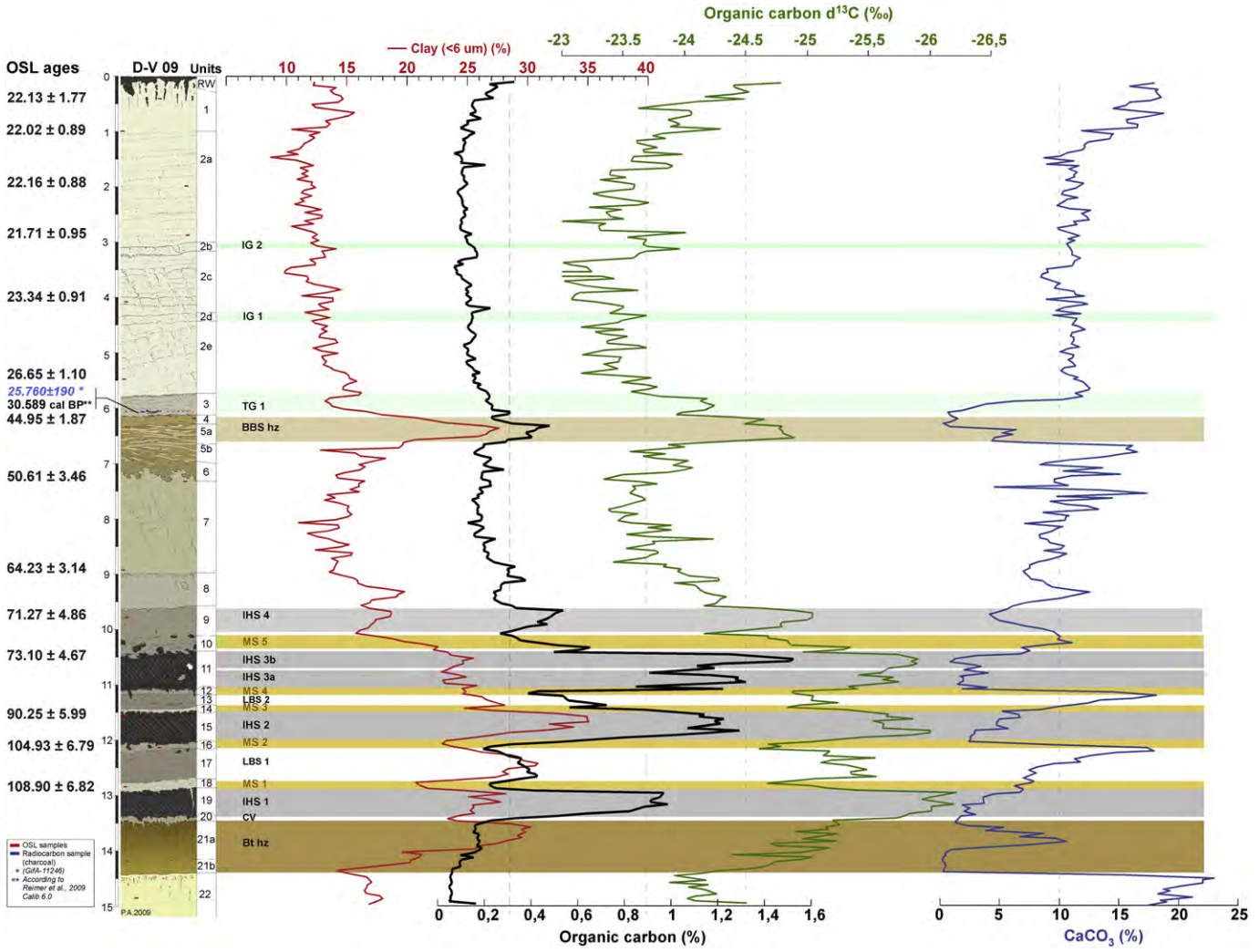

Fig. 6. Clay, organic carbon and $CaCO_3$ percentages, total organic carbon $\delta^{13}C$, OSL (quartz) & ^{14}C (charcoal) dates (^{14}C was performed on the AAA-resistant residue (Hatté et al., 2001b) and the humic acid fraction).

age (unit 22, $n = 11$) all show similar χ of $12.4 \pm 1.6 \times 10^{-8}$ m^3/kg, $14.7 \pm 1.7 \times 10^{-8}$ m^3/kg, and $12.4 \pm 1.0 \times 10^{-8}$ m^3/kg, respectively. Sub-sequence III brown soil (units 6–4, $n = 25$) as a whole displays a similar mean χ of $14.5 \pm 2.4 \times 10^{-8}$ m^3/kg with a net peak mean value through units 5a and 4 ($n = 8$) of $17.6 \pm 0.5 \times 10^{-8}$ m^3/kg. Unit 21 and sub-sequence I ($n = 96$) together, display a series of six peaks and troughs resulting in wide spread of χ values with a mean and standard deviation of $34.1 \pm 10.9 \times 10^{-8}$ m^3/kg. The highest value of 58.8×10^{-8} m^3/kg is reached in IHS 2 (unit 15). Low values, yet higher than in loess units, are observed in the thin silt layers of aeolian or colluvial origin (MS1 through MS5). The mass-normalized bulk magnetic susceptibility profile presented in Figs. 5 and 11 yields very similar intensities and variations with depth to previously reported data (Shi et al., 2003; Bábek et al., 2011) (in-field measurements); (Forster et al., 1996; Oches and Banerjee, 1996) (parts of our sub-sequence I) obtained along profiles at the brickyard site but at different sampling resolutions. Overall, variations follow the general trend observed in other European and Chinese loess sequences with higher χ in palaeosol (especially in humic & clayey horizons) with respect to loess related to in-situ mineralization of iron oxides during soil forming processes.

4.5. Organic carbon, $\delta^{13}C$ and $CaCO_3$

Comparison between the determination of $CaCO_3$ using CHN analyser and by the classical calcimetry (HCl) has been done for a set of 12 test samples.

As shown by comparing results from Table ii – Supplementary Material and Fig. 6, the wet leaching yields higher carbonate level than the calcimetry method. This likely results from both loss of iron oxides during wet leaching which artificially lowers the weight of remaining sediment and the assumption that all carbonates are solely under the $CaCO_3$ form (no dolomite). Wet soft leaching is preferred to dry drastic leaching to favour preservation of lipid and other complex component rather than amino acid. As amino acid in such old, arid and cold sediments should not be found anymore after several thousand of years, residuals amino acids that can be found at the analyses times, are definitively not linked to original organic matter but likely derives from modern organic matter that was later introduced in the field or in the lab. The choice of wet leaching is deliberate and adequate for the purpose of a palaeoclimatological study (it would not be the case for a pedological study). Nitrogen evaluation concomitant to carbon content evaluation is further used to evaluate such a contamination risk.

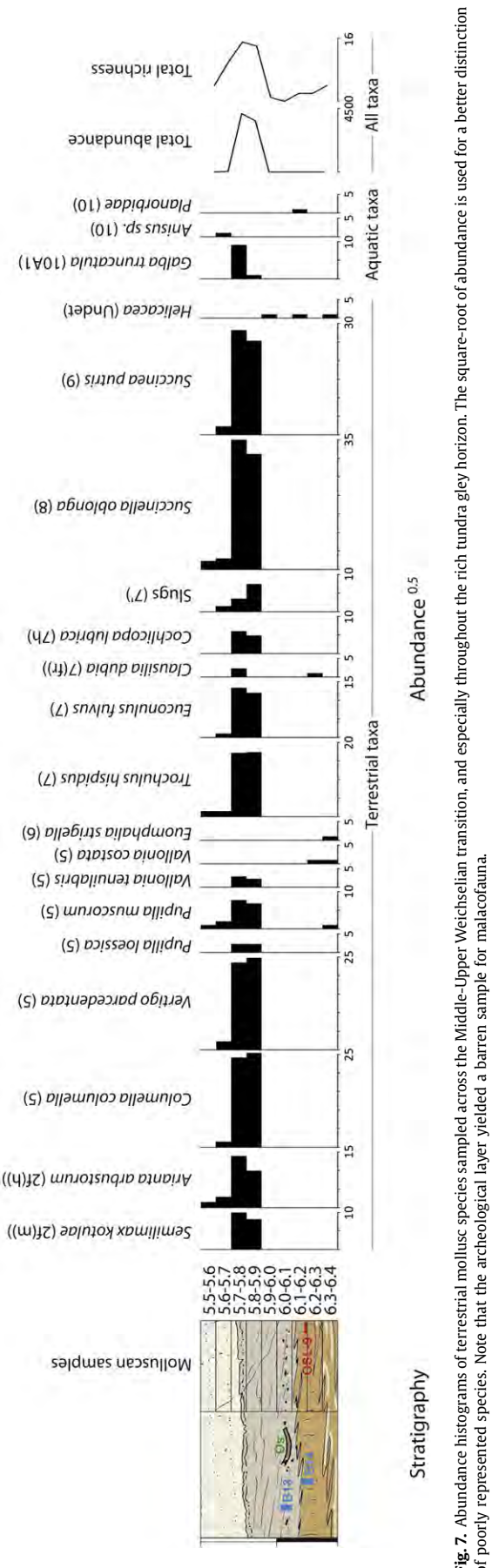

Fig. 7. Abundance histograms of terrestrial mollusc species sampled across the Middle-Upper Weichselian transition, and especially throughout the rich tundra gley horizon. The square-root of abundance is used for a better distinction of poorly represented species. Note that the archeological layer yielded a barren sample for malacofauna.

As commonly observed in NW European loess sections and presented in Fig. 6, organic carbon content remains very low during the glacial periods with a mean value lower than 0.1% wt associated to a carbonate content of ca 10%. The brown soil horizons of units 4 and 5a present slighter higher values of ca 0.4% wt associated to carbonate leaching. Palaeosols within the BHSC units show much higher organic carbon content reaching 1.4% wt, a value greater than that of the modern soil.

Likewise, organic $\delta^{13}C$ shows typical isotopic values for north-western European loess with $\delta^{13}C$ ranging from $-26‰$ recorded in IHS layers of the BHSC to $-23‰$ during glacial times with a decrease to $-25‰$ through the BBS.

The lower part of the section (from unit 9–21) presents a bouncing profile with values as low as $-26‰$ for units 11, 15 and 19 with higher values, reaching $-24.5‰$, for units 10, 12, 14, 16 and 18. The Corg profile mirrors the $\delta^{13}C$ bouncing profile with very high organic content reaching 1.2 %wt. This leads for higher vegetation productivity associated to wetter episodes.

4.6. Terrestrial molluscs

Mollusc species identified in the two basal samples located at the top of the brown soil complex in units 5a and 4 (Fig. 7, Table iii – Supplementary Material) are indicative of a locally dry and sunny environment with open vegetation. At the base of the tundra gley, the sample corresponding to the archeological layer (6.0–6.1) is sterile as are bracketing samples due to a strong decalcification of the sediment (Fig. 7). The rich and abundant malacofauna of the upper half of unit 3, dominated by *Columella columella*, *Vertigo parcedentata*, *Succinella oblonga*, and *Succinea putris* and including regional alpine species such as *Semilimax kotulae*, are characteristic of cold and humid conditions, with *in situ* shrub tundra vegetation (high proportions in *Arianta arbustorum*, *Euconulus fulvus* and *Trochulus hispidus*) and an increase in humidity at the very top of this horizon, where aquatic species *Galba truncatula* reaches its maximum abundance. In addition, dominant species *Succinella oblonga* (hygrophilous) and *Succinea putris* (palustral) indicate the presence of standing waters and/or of small water flows. Moreover, high species abundances and high proportions in juveniles of well represented species suggest a wealthier malacofauna than during loess deposition phases. Among this rich malacofauna and despite large abundances in *Vertigo* specimens, we did not observe the rare and badly known mollusc *Vertigo heldi* observed by Ložek (1953) and identified by Kovanda (1979) on the same material. The distribution of *V. heldi* being rather cryptic, its absence here may be due to the fact that it has been identified in a previous archaeological excavation located about 2 km to the SE of the presently studied section, where the orientation of the slope at the foot of Pavlov was not the same, inducing a different environmental setting. In the sample located at the base of loess unit 2e, the intermediate richness of malacofauna partly results from shells reworked from the underlying tundra gley horizon and that belong to the best represented species. Its malacofauna, as that of the uppermost sample, reflects a poorly vegetated environment with some persisting shrubs (*Arianta arbustorum*) and a somewhat humid (*Succinella oblonga*) character.

5. Synthesis and discussion

The high-resolution pedo-stratigraphy and analytical data presented herein and new OSL age determinations (Fuchs et al., 2012) provide sufficient insight to propose an updated pedosedimentary and palaeoenvironmental evolution of the Dolní Věstonice loess and palaeosol sequence of Last Interglacial–Glacial cycle in Central Europe. The occurrence of well preserved soil horizons and distinct changes in facies distinguish four main sub-sequences to the DV09

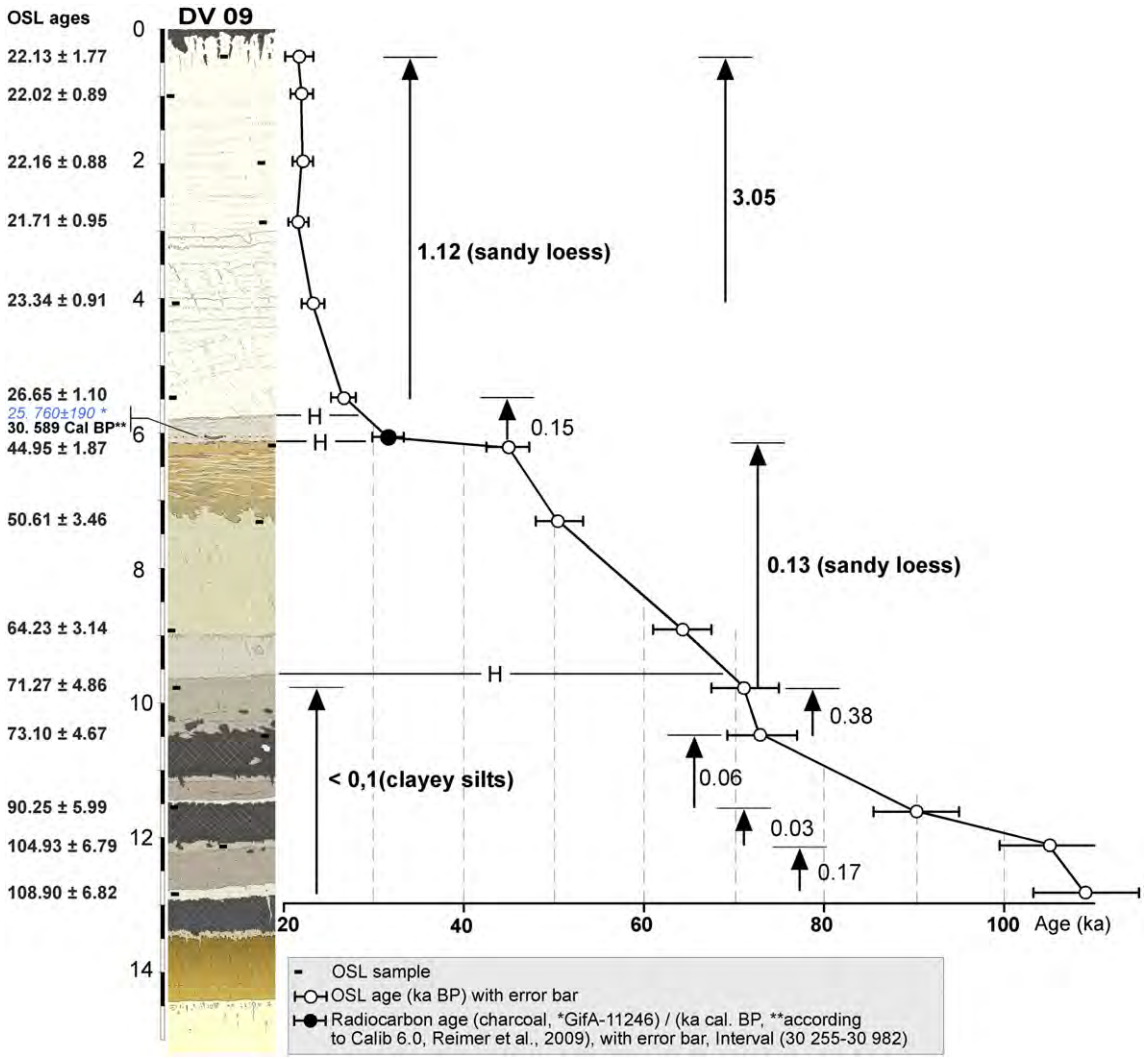

Fig. 8. Variations of the sedimentation rates and pedo-sedimentary balance along the profile according to OSL and ^{14}C dates.

record. These sub-sequences can be correlated to the main subdivisions and boundaries identified in other Upper Pleistocene loess-palaeosol records in Europe (Antoine et al., 2001, 2003a,b, 2009a,b; Horvath, 2001; Haesaerts et al., 2003; Novothny et al., 2011; Stevens et al., 2011). However, OSL ages and data presented here confirm that the DV loess-palaeosol sequence cannot be considered as a continuous record of the Last Interglacial–Glacial climatic cycle. Evidence of important hiatuses are observed at the boundary between the Middle Pleniglacial brown soil complex and the Upper Pleniglacial loess at 6.15 m depth, and between units 8 and 9 at 9.6 m depth (Fig. 8). Moreover, Upper Pleniglacial sandy loess units exhibit very high sedimentation rates, up to 1 mm/a, between units 2a and 2e (4.5 m), and higher than 2 mm/a between 2a and 2c (3 m). These sedimentation rates are one order of magnitude higher than within the basal soil complex (unit 20 to 9) where sedimentation slowed to ± 0.1 mm/a. These sedimentation rates should be compared to those found in the region in order to put this more into context.

The presence of hiatuses and highly variable sedimentation rates (Fig. 8) inhibit a direct correlation of the entire DV09 record with global palaeoclimatic records. However, by segmenting the DV09 record such correlations can be explored. The basal humic soil complex (BHSC, between 9.6 m and 14.5 m) represents an extremely complete sedimentary budget and coupled to a coherent OSL data set a correlation can be proposed with Greenland ice cores (GRIP Members, 1993; NGRIP Members, 2004; Svensson et al., 2008), Iberian margin marine cores (Sánchez Goñi, 2006; Martrat et al., 2007) and the NALPS speleothem record (Boch et al., 2011) (see Fig. 10). The Upper Pleniglacial loess (units 2 and 1) record is compared to other grain size records from Western Europe loess sequences (Antoine et al., 2009a) and to the GRIP dust record (Svensson et al., 2008).

5.1. Sub-sequence 1: basal humic soil complex (BHSC)

At the base of the DV section, the main feature of interest is the exceptionally well preserved thick soil complex encompassing units 21 to 9 (~5 m in thickness) and corresponding to Kukla (1975) PK III and PK II pedocomplexes (Fig. 2).

Immediately underlying the BHSC is unit 21, a truncated Bt horizon of a brown leached soil characterised by a high clay content (Figs. 6 and 11), a strong compactness, a brown–orange colour and a marked prismatic structure. Its location within the sequence, its pedological characteristics and the OSL age of the overlying unit 18 (108.9 ± 6.62 ka), suggest that this soil horizon developed during the Last Interglacial (Eemian – MIS 5e). The Eemian soil (unit 21)

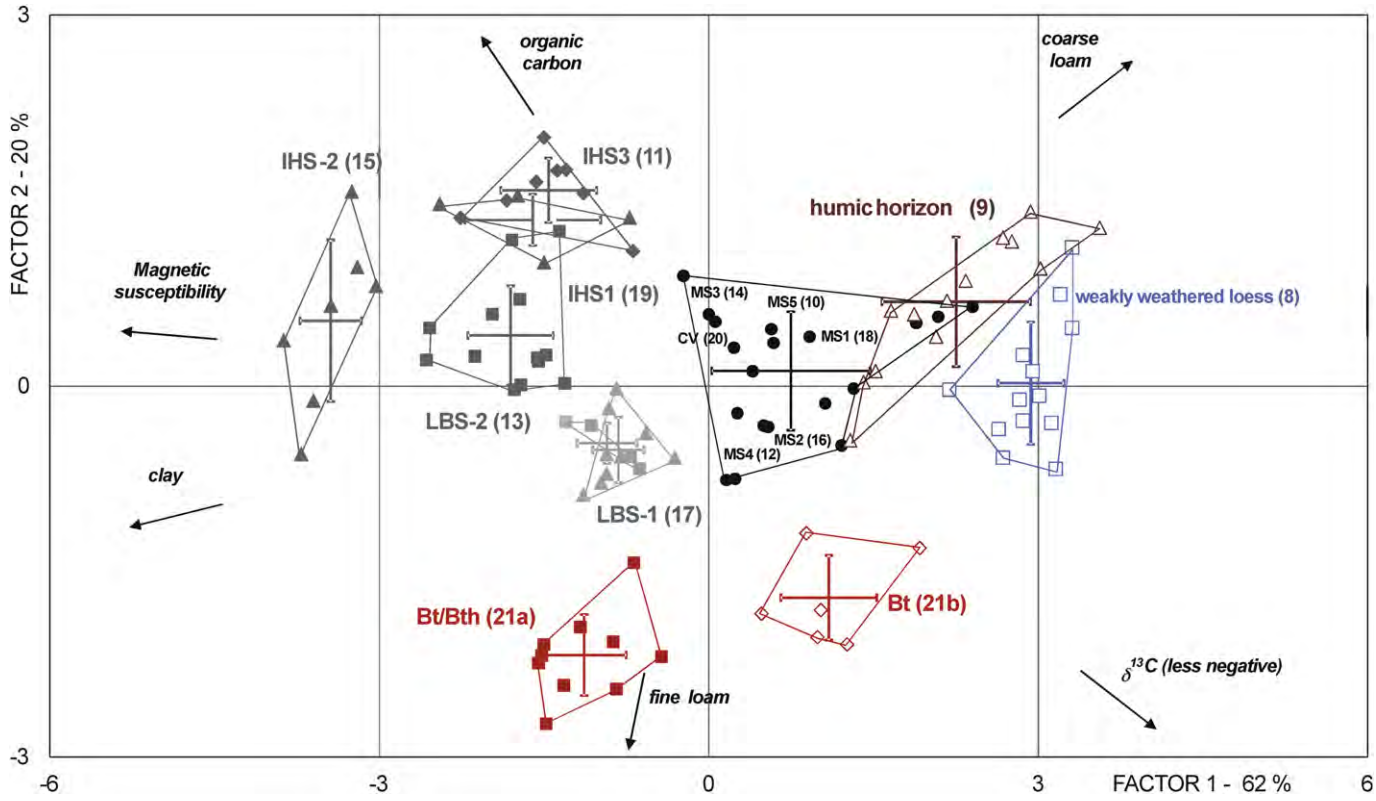

Fig. 9. Principal component analysis (PCA) of the Early-glacial humic soil complex and Interglacial horizon of the Dolní Věstonice sequence (106 samples). The cross inside a group represents the mean point $\pm 1\sigma$. Bt/Bth: upper horizon of the interglacial soil, The first axis discriminates the sediments according to the grain-size (coarse silt vs. clay), $\delta^{13}C$, which opposes humid and arid conditions, and the magnetic susceptibility and organic carbon, which are mainly representative of the intensity of soil weathering. The second axis makes a distinction between the grain size (fine silt vs. coarse silt) and, in a lesser part from the first axis, between organic carbon content and aridity ($\delta^{13}C$ less negative). In this figure units characterised by stronger weathering and pedogenesis processes are localized in the left side of the first factor (high values in TOC, clay, χ and less negative $\delta^{13}C$). This diagram allows to split a statistical population into several groups with specific grain size, magnetic and geochemical properties, and the discrimination of the respective weight of the various variables inside these groups. The two first factors explain respectively 62 and 20 % of the variance. Six variables are considered in the PCA analysis: clay %, fine silt %, and coarse silt %, magnetic susceptibility, organic carbon % and organic carbon $\delta^{13}C$ ‰. The main interpretations from the PCA analysis are discussed in Part 5. An analysis on all 300 samples resulted in a rainbow "gutman" effect (Van der Maarel, 1980) providing little additional information to the more discriminant representation of the whole data set in the ternary diagram of Fig. 4.

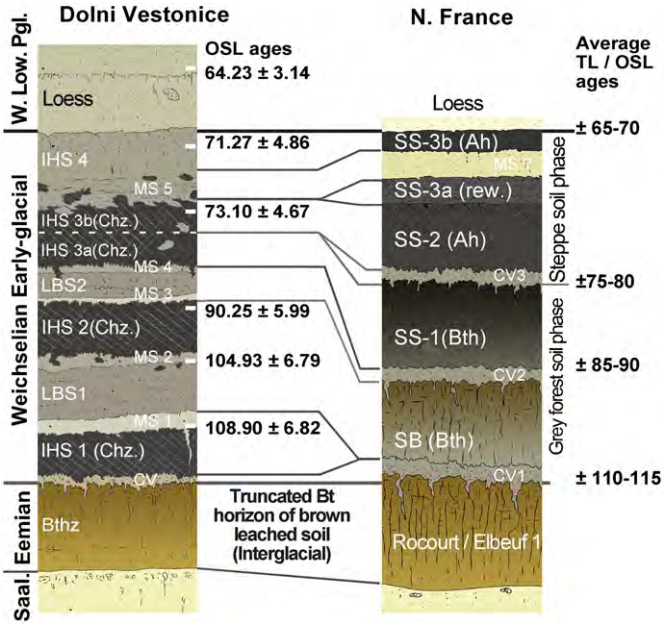

Fig. 10. Correlation between the Weichselian Early-glacial humic soil complex from Dolní Věstonice and Northern France (data for Northern France: according to Antoine et al., 1999a,b, 2003a,b).

overlies a typical calcareous loess horizon (unit 22) that can thus be allocated to the Late Saalian (MIS 6) even though the OSL age of BT 752 greatly underestimates the true burial age. OSL age underestimation within Saalian loess is frequently observed in other European loess records (Frechen et al., 1999).

Thin section analysis reveals that unit 21 is a complex Bt horizon including two distinct generations of clay coatings. The first generation is characterized by pale yellow weakly stratified clay coatings while the second generation is characterized by stratified dark, humic clay coatings (Fig. 3A,B & Table i – Supplementary Material). The second generation corresponds to the development of a grey forest soil (boreal forest) indicating a more continental climatic phase, post dating the full interglacial and occurring after a desiccation event (prismatic feature/desiccation cracks). This complex Bt horizon is also characterised by high χ values and clay content, close to those observed in IHS 1 (Fig. 5). Finally, a phase of secondary carbonate impregnation (nodules) is observed in the upper part of unit 21a ($CaCO_3$ up to 10%, Fig. 6). Considering that the formation of the Bt horizon induced a full decalcification during the interglacial, these secondary carbonates likely originate from a younger period of pedogenic alteration related to the development of the directly overlying humic soil IHS 1. The distinction between units 21a and 21b observed during field works and in thin sections (Table i – Supplementary Material) is also reinforced by PCA analysis in which they occur as clearly separated groups (Fig. 9).

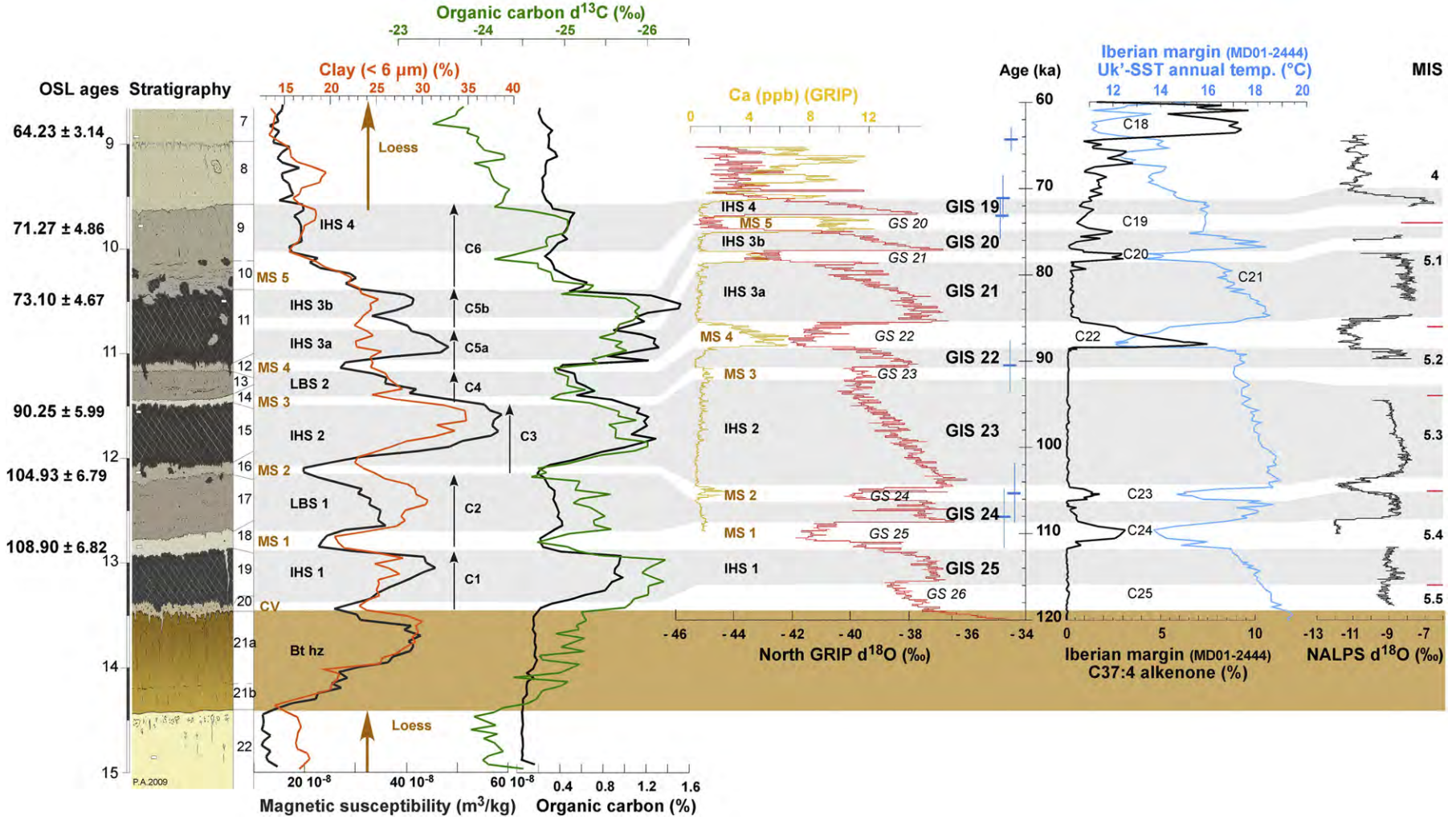

Fig. 11. Correlation proposed between the DV basal soil complex and the North GRIP $\delta^{18}O$, GRIP dust (NGRIP Members, 2004; Andersen et al., 2006), Iberian Margin sea surface temperature (Martrat et al., 2007; Guihou et al., 2011) and NALPS $\delta^{18}O$ records (Boch et al., 2011) between 60 and 115 ka.

An erosional surface truncates the Eemian Bt soil and is topped by unit 20, a thin layer of clayey colluvial deposit (CV) which includes soil nodules and Fe–Mn concretions (1–2 mm) derived from unit 21b (Fig. 3C). This erosional surface has been observed, for example, by Frechen et al. (1999) who described the discontinuity as being associated with a discontinuous gravel bed. The molluscan record of Ložek (1953) sampled the colluvial of unit 20 and lower half of IHS 1 of unit 19 as a single sample preventing a segregation of the environmental conditions prevailing during the deposition and the development, respectively, of the these two units. A single fragment of *Helix pomatia*, typical of warm and humid interglacial conditions, was found in this sample and thought to result from a reworking process (Klima et al., 1962). All the data thus show that there is a main shift between units 21a and 20 before and after the erosional surface at the top of the Bt horizon of unit 21a.

Overlying the erosional event, the BHSC (Subsequence 1) is composed of a succession of black clayey-humic soil horizons (units 19, 15 & 11) a greyish humic horizon (unit 9), homogeneous calcareous silts ("marker silts": units 18, 16, 14, 12 & 10), and dark brown clayey humic horizons (units 17 & 13). The BHSC is interpreted as a succession of 6 pedosedimentary cycles, each starting with a sedimentation event and ending with the formation of a soil (cycles 1 to 6: Figs. 2 and 11). Cycle 5 has been divided in two subcycles 5a and 5b on the basis of analytical data (TOC, $\delta^{13}C$, $CaCO_3$, χ, clay) that clearly show that IHS 3 is actually composed of two soil units (IHS 3a & 3b, Figs. 5 and 6) separated by a weak aeolian sedimentation phase. Cycle 6 is composed of the last marker silt unit (MS 5) which is partly reworked due to the presence of laminations and bioturbation and topped by a weakly developed dark grey isohumic soil horizon (IHS 4).

5.1.1. Isohumic soils (IHS)

The three main humic "black soil" horizons (IHS 1, 2 and 3) show very similar characteristics both in field and thin section analysis. They are homogeneous, dark in colour, presenting an isotropic clayey-organic complex (plasma), strongly bioturbated resulting in a deep incorporation of organic matter (organic micro-debris, numerous dark micro-aggregates <50 μm, humified vegetal remains, faecal pellets) and have precipitates of $CaCO_3$ in the form of calcium carbonate hard nodules, very dense fine root track network <1 mm, carbonate coatings around bio-pores and needle-shaped calcite crystals (Fig. 3E,F,I). The above characteristics combined to a clay content of 25–30%, an organic carbon content of 0.6–1.5% and up to 5% of secondary carbonate are consistent with a haplic chernozem soil (*chernic*) horizons (Gerasimova et al., 1996; WRB, 1998; Gerasimova, 2003; Eckmeier et al., 2007). The abundant black micro debris observed in thin section within the clayey-organic plasma could be linked to charred organic carbon resulting from natural fires, as described in some German Holocene chernozems (Schmidt et al., 1999). This hypothesis could explain the very high amount of TOC that characterises the chernozem horizons at DV compared to present-day analogues (Gerasimova, 2003). The PCA analysis (Fig. 9) of the chernozem soils (units 11, 15, and 19) shows that they are the most weathered facies of the sequence with the highest χ values and organic carbon content and the finer grain sizes and among them IHS 2 has undergone the highest degree of pedogenic alteration and IHS 4 the lowest within the BHSC.

The malacofauna assemblage of the chernozems of the BHSC is composed of xerophilous taxa (*Granaria frumentum*, *Chondrula tridens*, *Helicopsis striata*), open environment taxa (*Pupilla muscorum*, *Pupilla loessica*, *Vallonia costata*, *Vertigo pygmaea*) and hygrophilous taxa (*Succinea*/*Succinella* sp.) (Klima et al., 1962) suggesting that IHS 1, 2 and 3 developed in a temperate continental climate with a herbaceous vegetation disseminated by forested patches (i.e., a forest-steppe soil). The poverty and the similarity of malacofauna within the IHS horizons prevent any reliable palaeoenvironmental differentiation between these units. However, the assemblages due differ between the two sub-soils in IHS 3. The upper half of unit 11 is composed of *Pupilla muscorum*, *Helicopsis striata* and *Euomphalia strigella* (Klima et al., 1962), reflecting a drier (absence of *Succinea*/*Succinella* taxa) and colder (absence of typical steppe taxa) environment with a bushy and poorly herbaceous vegetation. The youngest humic soil horizon (IHS 4/unit 9) is dominated by species such as *Vallonia costata, Helicopsis striata*, *Pupilla triplicata* and slugs indicative of dry and moderately cold, yet warmer than through IHS 3b, herbaceous steppe (Klima et al., 1962). IHS 4 shows the least developed pedogenesis especially with regards to clay content and to a lesser extent $\delta^{13}C$ that only marks a slight climatic improvement in a general trend of aridification.

5.1.2. Lehmbröckelsand soils (LBS)

Intercalated between the dark chernozem IHS 1, 2 and 3 of the BHSC are two massive greyish brown clayey-organic horizons (units 17 and 13), referred to as "Lehmbröckelsand" and interpreted as colluvium in a temperate continental environment (Kukla, 1977). Our sedimentological data (field observations, grain size, and thin sections), demonstrate that these layer do not only result from colluvial sedimentary events but also exhibit a pedological imprint, which is weaker but not very different from that of chernozem horizons. For example, the thin section analysis of LBS 1 (unit 17) shows a strongly bioturbated structure, primary carbonate grains, humified vegetal debris (±50 μm), calcified root cells, calcite needles in biopores, and also clay formed *in situ* underlined by evidence of weathering of the surface of carbonate grains (Fig. 3H). At the thin section scale of observation, the pedological imprint has almost totally destroyed the initial colluvial sedimentary structure. Evidence of the colluvial deposition processes is however weakly observed as discontinuous laminations in the field (sample B4, Fig. 2). Even if LBS 1 and 2 likely correspond to shorter interstadial events than IHS 2 and 3, these new results are very important because they show that the record of the BHSC of DV has recorded more interstadial events than previously thought.

An environmental differentiation can be proposed on the basis of molluscan data presented in Klima et al. (1962). The malacofauna of LBS 2 (unit 13) reflects the same environmental conditions than those of chernozem soils, whereas species of the lower half of LBS 1 indicate drier and colder conditions. The assemblage in the lower half of LBS1 is very similar to that within the underlying aeolian silt MS 1 (unit 18) either due to reworking, or persistence, of *Pupilla triplicata* which are very abundant in MS 1. The malacofauna of the upper half of LBS 1 is composed of *Trochulus hispidus* and *Arianta arbustorum* suggesting slightly cooler and more humid conditions intermediate between conditions prevailing during the formation of IHS 1, 2 and 3.

5.1.3. Marker silt layers (MS)

Within the BHSC, several thin (5–10 cm thick) aeolian calcareous silts units, called marker silt (MS), have been identified (units 10, 12, 14, 16 and 18). These layers, especially unit 18, are characterised by a very homogeneous texture (Fig. 3G), a light-brown colour, a well-sorted coarse silt grain size distribution, a 5–20% $CaCO_3$ content, and a relatively high TOC content (0.2%) compared to loess. The PCA analysis clearly differentiated the MS from loess units 22, 8, 7, 2 and 1 (Fig. 9).

Thin sections from unit 18 show evidence of abundant well sorted primary carbonate grains (between 30 and 50 μm), secondary carbonates (hypocoatings) and ubiquitous bioturbation burrows (2–3 mm in diameter) filled with darker humic material

from IHS 1 and LBS 1. The occurrence of this fine bioturbation network (earthworm burrows) has to be taken into account for the interpretation of the relatively high TOC content of the marker silts. The thicker MS units 18 and 16 have TOC content of ~0.2% whereas the thinner MS units 14 and 12 have TOC content ranging between 0.4 and 0.6%. The latter are more impacted by bioturbation.

On Fig. 9, the various marker silts appear close to the origin of the factorial plan, in a badly defined intermediate position between humic and clayey soils, and the weakly weathered loess. In addition, MS 2 and MS 4 (units 16 and 12) show characteristics close to that of the underlying LBS units (high amounts of fine silt), while MS 1 (unit 18) is definitely richer in coarse silt. Finally, MS 3 and MS 5 appear more weathered likely because of the inclusion of particles reworked from the bracketing humic soils (bioturbation).

Mollusc species identified by Klima et al. (1962) within the marker silt layers are varied. MS 2 and MS 5 yielded few counts but their assemblages closely resemble those of the chernozem soils (IHS 1, 2 and 3a). MS 1 is dominated by *Pupilla triplicata* indicative of very dry but moderately cold conditions. A single sample in Klima et al. (1962) encompasses MS 4, LBS 2 and MS 2 hindering an environmental differentiation between these units. However, this sample yielded *Pupilla loessica*, a species also present at the base of IHS 3b (unit 11), suggesting this specie appeared in MS 4. The presence of *Pupilla loessica* is compatible with a colder climate than during the deposition of MS 1.

The marker silts are considered to be aeolian in origin and more specifically associated to dust storm events occurring in a continental steppe environment (Kukla, 1977). In this type of environment, soil dust could have been produced during storm events by deflating chernozem topsoils in areas where the vegetation cover is sparse due to, for example, climate deterioration or natural fires (continental dry climate). The marker silts thus differ in their origin from typical periglacial loess. The latter considered to result from the deflation of extensive detrital sediment sources (e.g. braided rivers) (Antoine et al., 2009a) producing thick loess deposits. When proximal to major river systems, loess may include an important sand component (Smalley et al., 2009) as is the case in DV where fine sand content may reach 20–30%. The marker silts, while aeolian, differ from the loess of units 22, 8, 7, 2 and 1 in its silicate mineral content. Microscopic observations reveal that the MS have a significantly lower amount of micaceous particles which are ubiquitous in the loess.

Pending questions are: What is the source of the MS sediment and what distance has the material travelled? Such marker silts are not observed in western European Early-glacial soil complexes other than in Achenheim (Rousseau et al., 1998a,b). Similar silt layers have been observed in Ukraine (Rousseau et al., 2001; Gerasimenko, 2006; Gerasimenko and Rousseau, 2008) suggesting that their origin is likely related to a continental scale process restricted to Central Europe as formerly proposed by Kukla (1977). Additional insight is provided by Cilek (2001) who found in MS 5 a heavy mineral assemblage compatible with crystalline complexes of the Bohemian–Moravian highlands located about 100 km west of DV.

5.1.4. Comparison between BHSC of DV09 and western European records

The comparison of the DV basal soil complex with pedosedimentary records from Northern France, Belgium or Germany (Antoine et al., 1999a, 2001, 2003a,b, 2009a; Haesaerts et al., 1999; Haesaerts and Mestdagh, 2000; Schirmer, 2000; Frechen et al., 2001; Meijs, 2002) (Fig. 10) lead to the following observations:

1) The humic black soil horizons of DV09 are characterised by the absence of laminated organic-clay coatings generally found in grey forest soils developed during the same period in Western Europe.
2) Chernozems develop throughout the Early-glacial period at DV while in Western Europe grey forest soils topped by steppe soils are formed. Aeolian horizons are interbedded between chernozem in DV09 while the only aeolian event recorded in Western Europe is at the top the very end of the Early-glacial period (Fig.10).
3) Hydromorphic features (glossic horizons, oxidation) are not observed at the top of the various soil horizons in DV09 while ubiquitous in Western Europe. The absence of hydromorphic features is indicative of dry conditions which supports the conclusion in (1) of a drier climate at DV with respect to Western Europe at the same time period.

From these observations, one may conclude that the climate during the formation of the BHSC in Moravia was markedly drier than in other parts of Europe during the Weichselian Early-glacial including the Ukraine where grey forest soils are described at the base of the contemporaneous Pryluki Early-glacial soil complex (Rousseau et al., 2001; Gerasimenko, 2006; Gerasimenko and Rousseau, 2008). During the Last Interglacial, all of Europe endured an oceanic temperate climate and developed brown leached soils with Bt horizons (unit 21b at DV). The grey forest soil phase registered in the upper part of the Bt horizon at DV (unit 21a, Table i – Supplementary Material) indicates an evolution towards continental climatic conditions at the end of the Eemian. Elsewhere in Western Europe this shift was delayed to the first interstadial of the Weichselian Early-glacial (MIS 5c).

In summary, the DV BHSC is one of the most complete pedosedimentary record of continental environmental and climatic changes between about 110 and 70 ka (Fig. 11) encompassing 6 cold phases represented by a colluvial deposit (unit 20) and 5 aeolian events (marker silts of unit 18, 16, 14, 12 & 10) and interbedded within 7 interstadial events represented by soil horizons (units 19, 17, 15, 13, 11a-b, 9).

5.1.5. Comparison between BHSC of DV09 and global palaeoclimate records

OSL results (Fuchs et al., 2012) indicate that the BHSC developed during the Weichselian Early-glacial between about 110 and 73 ka and is thus contemporaneous to the main interstadials of MIS 5c to 5a of marine records (Shackleton et al., 2002, 2003; Lisiecki and Raymo, 2005; Sánchez Goñi, 2006). Given that seven soils developed during this time period the two main interstadials within this period (MIS 5a and 5c) cannot be correlated to a single palaeosol of the DV BHSC. However, the analytical data (TOC, χ, clay and $\delta^{13}C$) shows that IHS 2 has the highest degree of pedogenic alteration which logically could be associated to the longest interstadial period of MIS 5c (or MIS 5.3 peak at 96 ka in Lisiecki and Raymo (2005)). OSL ages corroborate the correlation of IHS 2 to MIS 5c.

Fig. 11 proposes a set of correlations between clay content, χ, TOC and $\delta^{13}C$ record, and global palaeoclimatic records of Greenland $\delta^{18}O$ and dust (GRIP Members, 1993; NGRIP Members, 2004), Iberian Margin high resolution marine cores (Shackleton et al., 2000, 2004; Sánchez Goñi, 2006; Martrat et al., 2007) and NALPS $\delta^{18}O$ (Boch et al., 2011).

Isohumic palaeosols (IHS) 1, 2, 3a, 3b and 4 developed during Greenland Interstadials Stage (GIS) 25, 23, 21, 20 and 19 respectively. Lehmbröckelsand palaeosols (LBS) 1 and 2 developed during GIS 24 and 22 respectively. If the magnitude of χ is directly propositional to the degree of pedogenesis then the 7 palaeosols of the BSHC would be ranked from least to most developed as follows: IHS 4, LBS 2, LBS 1, IHS 3b, IHS 1, IHS 3a and IHS 2. Based on the North GRIP $\delta^{18}O$ data, the length of the GIS events are in perfect

agreement with the least developed palaeosols forming over ~2 ka (IHS 4, LBS 2, LBS 1), ~3 ka (IHS 3b), ~4 ka (IHS 1), ~7 ka (IHS 3a) and finally ~12 ka (IHS 2). Such a correlation between degree of pedogenesis and time of soil formation is not as straight forward with TOC, clay content or $\delta^{13}C$.

The aeolian marker silt horizons are associated with cold stadials. The stratigraphic position and OSL age of MS 1 (109 ka) argue for a deposition during Greenland Stadial (GS) 25 equivalent to the first major cooling event (C24) in Iberian margin marine cores (Chapman and Shackleton, 1999). C24 also coincides with decreasing arboreal pollen percentages in the Füramoos pollen record in Southern Germany (Müller et al., 2003). MS 2 to 5 are then allocated to cold events C23 to C19 and to GS 24 to 21, the corresponding cooling and dust events in NGRIP (Fig. 11). The present day thickness of the various MS layers cannot be used as an indicator of the intensity of the aeolian events associated to the cold phases since this is dependent on the degree of pedogenesis of the overlying soil. C22 (GS22) is the longest cold event but is overlain by IHS 3a which is likely the second most developed palaeosol which results in the end with a thin ~5 cm thick MS 4.

5.2. Subsequence II: first loess deposition (~70–50 ka)

The transition between the BHSC and the first thick loess deposit (unit 8 and 7) occurs at ~9.6 m depth. The transition is characterized by a sharp drop in both organic $\delta^{13}C$ values and TOC content (Fig. 6) and an increase in sedimentation rates (Fig. 9). Fine sands increase most notably through unit 7, peaking at ~30%, concomitant with the observation of laminations dipping ± 10° northwards on a north–south trending sub-vertical face.

The sedimentological characteristics of unit 8 and 7 indicate an extremely arid climate with strong winds (storms) able to drift fine and coarse sands from proximal sources, likely the braided Dyje River valley located a few hundred metres North of the site. As to the provenance of the silt fraction, Lisa and Uher (2006) showed from zircon typology and cathodoluminescence that the source is located northwest of DV within the Bohemian massif. The laminations of unit 7 may reach a few millimetres in thickness and are composed of medium to coarse sand beds. They likely represent a succession of storm events as suggested by Cilek (2001) from observations in Moravian loess and by Antoine et al. (2001, 2009a) from observations in the Nussloch loess section in Germany.

Here we must underline that while grain size variations are often interpreted in terms of wind strength variations, some results of modelling studies (Alfaro and Gomes, 2001; Grini and Zender, 2004) suggest that grain size coarsening may result from the complex interplay of aridity, vegetation, grain size of the drifted material, dust transport (source area) distance and wind strength.

Nevertheless, the occurrence of abundant coarse sand grains in DV loess record during periglacial phases like the Lower or Upper Pleniglacial clearly indicate that the main sources for typical loess were located in the braided Dyje river valley.

Therefore, the source location did not change through time and, in this environment characterised by unstable sandy and gravely bars with no vegetation cover, the material (silt and sands) was homogenised by fluvial sediment mixing during extreme flooding events. Only changes in river system morphology may have induced grain size variations in the parent material. Indeed, periglacial braided river systems (Lower and Upper Pleniglacial) are characterised by a huge deflation, whereas meandering or stable multi-channel river systems (Early-glacial or Middle Pleniglacial) deflation surface and grain size are likely strongly reduced (absence of sand and gravel bars exposed to deflation). This is clearly shown at DV where the median grain size of the marker silts interstratified in the Early-glacial soil complex is markedly lower than in loess.

Finally, the interpretation of loess grain size signal in terms of wind strength variations is strongly supported by extremely close variation patterns (especially during Upper Pleniglacial) at DV and in other European loess sequences located in the Rhine Valley or in Northern France, more than 600 to 1000 km to the west (Antoine et al., 2009a,b).

The OSL age obtained at the base and top of unit 7 (Figs. 5 and 6) and its stratigraphic position leads to the attribution of units 8 and 7 to the Weichselian Lower Pleniglacial (±MIS 4). This period is the first main dust peak dated at 65–60 ka in NGRIP and corresponding to C18 cold event of Iberian margin marine records (Fig. 11). In Western European sequences, Lower Pleniglacial loess is rarely preserved or show very small thicknesses (Antoine et al., 2003a,b). The DV09 sedimentary budget is comparable to other Central European deposits such as the Ukrainian "Uday" loess (Gerasimenko, 2006; Gerasimenko and Rousseau, 2008) or the Serbian "VL1L2" loess (Marković et al., 2008; Antoine et al., 2009b).

5.3. The middle brown soil complex (subsequence 3): a highly condensed budget of the Middle Pleniglacial (~55–40 ka)

The contact between the Lower Pleniglacial sandy loess deposit and the middle brown soil complex is irregular and marked by intensive bioturbation processes such as burrowing. The complex encompasses units 6 to 4 from 7.30 to 6.15 m depth and corresponds to the lower half of PKI following the nomenclature in Kukla (1975). Pedologically, the complex is a boreal to Artic brown soil with unit 4 being clearly *in situ* while units 5a, 5b and 6 show features consistent with deformations induced by solifluction (frost creep).

Unit 6 corresponds to a boreal brown soil (Bw horizon of Cambisol) but it is strongly reworked and eroded by solifluction. The geomorphologic location of the profile downslope of the Pavlov Mountain can explain the local intensity of these processes. The association of *Trochulus hispidus* (mesophilous) and *Succinea putris* (palustral) reflects a poor vegetation cover and cold but more humid conditions than during the deposition of unit 7 (Ložek, in Klima et al., 1962).

Units 5a and 5b correspond to at least two distinct events of solifluction leading to an undulated layering of the horizon composed of alternating brown clayey beds of reworked soils and light grey calcareous silts ($CaCO_3$ up to 15% in 5b and 4–5% in 5a). Such a texture is known of intense freeze–thaw processes as previously postulated by Cilek (2001). All the measured parameters are very contrasted between units 5a and 5b, each having analytical data more similar to unit 4 and 6 respectively. Malacofauna in unit 5b are of the *Granaria frumentum, Pupilla triplicata, Vallonia costata, Succinella oblonga* and *Pupilla* species type suggesting warmer, more humid and herbaceous steppe environment (Klima et al., 1962) while in unit 5a the disappearance of *Succinella oblonga* (hygrophilous) and the replacement of steppic species *Granaria frumentum* and *Pupilla triplicata* by *Arianta arbustorum* and *Helicopsis striata* (common in loess) indicate lower humidity and colder conditions.

Lastly, unit 4 corresponds to a more or less *in situ* boreal to arctic brown soil horizon. Its upper and lower boundaries are irregular (tongue horizons) and its internal structure (thin undulated banded fabric) suggests weak slumping down the slope. The high density of unit 4 is characteristic of horizons compacted by frost-creep. The reworking observed in unit 4 is less important than in the underlying units 5a-b. The two species from the base of unit 4, *Vallonia costata* and *Clausilia dubia*, suggest an open, fairly humid and bushy vegetation (Table iii – Supplementary Material & Fig. 7), whereas the sample from the upper half is almost sterile due to decalcification.

The stratigraphic position of the middle brown soil complex sandwiched between two major loess horizons and the OSL age of ~51 ka at the top of unit 7 and of ~45 in unit 4 support the conclusion that this soil complex developed during the Middle Pleniglacial corresponding to GIS 14 to 12. However, the record is not continuous due to numerous hiatuses associated with gelifluction events and is highly compacted rendering any comparison with global palaeoclimate records inappropriate.

The DV brown soil complex is characterized by facies similar to that of the Middle Pleniglacial brown soil complexes of other European loess sequences such as the "Vytachiv" soil complex of Ukraine (Gerasimenko, 2006), the "Saint-Acheul–Villiers-Adam" soil complex in Northern France (Antoine et al., 2003a,b), the Gräselberger and Löhner Boden in Germany (Antoine et al., 2009a) the Gleina soil complex (Meszner et al., 2011) and the Willendorf soils in Austria (Haesaerts et al., 1996, 2003). If one considers that the soil of unit 6 is *in situ*, it could be contemporaneous to the basal part of the Bohunice soil in Czech Republic (Valoch, 1976) dated at ~45–50 ka (Richter et al., 2009).

5.4. Tundra gley and upper sandy loess units (subsequence 4) (~30–20 ka)

Subsequence 4 represents the upper 6 m of DV09. A tundra gley horizon some 40 cm thick hosting the Gravettian archeological layer underlies 4.5 m of sandy loess of unit 2 and 1 m of loess of unit 1.

5.4.1. Tundra gley (TG1) and archaeological layer

The tundra gley, a gelic gleysol (unit 3) underwent strong solifluction processes (frost creep) resulting in the occurrence of thin, discontinuous undulated iron oxide bands throughout the unit. As generally observed in gleyed loess horizons, χ values are among the lowest, clay content is slightly higher than in loess (10–12% in loess compared to 15% in the tundra gley) and $CaCO_3$ is depleted (secondary carbonate concretion). The loessic origin of the gleyed sediment of unit 3 is confirmed by the fine sand content reaching 35%, similar to values throughout the overlying loess of unit 2.

The Gravettian archaeological layer intercepted at 6.10 to 6.00 m depth during the preparation of DV09 likely corresponds to the level excavated in the 1960's by Klima et al. (1962). A fragment of mammoth bone (rib) and a rich charcoal layer were re-discovered. New radiocarbon ages on extracted charcoal yielded an uncalibrated radiocarbon age of 25 760 ± 190 BP, GifA-11246 (30 589 cal BP). This is quite younger than uncalibrated ages previously published on charcoal by Klima et al. (1962) (29 000 ± 200 ^{14}C BP and 27 660 ± 80 ^{14}C BP). The discrepancy between ages is difficult to assess. However, various authors have shown that the Gravettian layers from archeological sites in DV (I & II), Pavlov and Mirovice, extending on several kilometres along the Dyje River at the base of the Pavlov Mountain, have yielded a wide range of uncalibrated ^{14}C ages from about 25.5 to 28.5 ka (Damblon and Haesaerts, 1997; Svoboda, 2001; Beresford-Jones et al., 2011). Thus, the charcoal layer dated in this study probably corresponds to the youngest human occupation of the area and is likely contemporaneous of the human burial DVII (XVI) dated at 25.570 ^{14}C BP (Beresford-Jones et al., 2011). Consequently, whatever the selected results, radiocarbon ages confirm the occurrence of a huge hiatus in the record between the top of the brown soil and the tundra gley layer (likely 10–15 ka). The occurrence of this hiatus is also clearly expressed when comparing DV09 to other sequences, such as Nussloch, which are characterised by a more complete sedimentary budget of the base of the Upper Pleniglacial (Fig. 12). This hiatus has also been widely evidenced in European loess records (Haesaerts and Mestdagh, 2000; Meszner et al., 2011; Antoine et al., 1999a, 2003a,b).

Pollen analysis within the Gravettian archeological layer is composed of 30–70% of arboreal pollen dominated by *Pinus, Picea, Juniperus* and *Larix*, with occurrence of oak, hazel and beech (Svoboda, 1991; Svoboda, 1995) is indicative of a continental climatic regime favourable to the development of trees. The occurrence of conifer trees in Moravia is also demonstrated by charcoals (Beresford-Jones et al., 2011) and, over the same time period, at Willendorf in Lower Austria (Damblon and Haesaerts, 1997). The presence of large mammal suggests a more open landscape, described as a Mammoth-steppe environment by Guthrie (2001), which is coherent with the cold-adapted conifer assemblage (*Pinus, Abies, Larix/Picea* & *Juniperus*) inferred from pollen analysis and charcoals mentioned above. The landscape at the time of human occupation near DV was likely a composite with trees restricted to protected downslope positions and open plateaus covered with steppe vegetation.

The malacofauna analysis of unit 3 (Fig. 7) yielded species, in the upper part of the unit, indicative of a tundra environment. The lower half of the unit is barren of shells due to an almost complete decalcification of the horizon. Therefore, our data do not permit a palaeoenvironmental reconstruction for the time period of human occupation. However, others at other locations have identified species consistent with cold and humid conditions within the tundra gley and associated with the archeological layer (Petrbok, 1951a,b; Ložek, 1953; Kovanda, 1991). One must keep in mind, that the base of unit 3 does show iron oxide banding suggesting some degree of reworking due to water logging processes casting some doubts as to the true stratigraphic origin of the shells. This said the extent of gley related reworking would be site dependent as a function of the geomorphic position of the profile.

In western Europe, mollusc assemblages associated with cryoturbated tundra gley horizons show an increase in humidity-seeking species, a decrease in the diversity of species due to increasing humidity and a strong increase in abundance. These observations are interpreted as a response to warmer interstadial conditions (Moine et al., 2008, 2011). At DV09, within TG1, humidity-seeking species increase, overall abundances increase, characterized by a higher proportion of juvenile individuals, but the diversity of species also increases instead of decreasing as expected. This discrepancy may be a site dependent effect related to the slope position of DV09 favouring a lateral drainage of infiltrating waters facilitating hillwash processes and limiting harmful effects of water logging on the molluscan record. A secondary effect of water logging and ice-lense formation is a reduction in the vegetation cover leading to a decrease in vegetation-seeking mollusc species as observed, for example, in Nussloch tundra gleys (Moine et al., 2008) but not here in TG1 of DV09.

In summary, the formation and degradation of TG1 results from an interstadial warming phase that enhanced the seasonal degradation of the permafrost active layer leading to solifluction related deformation and alteration of the horizon. The OSL age at the base of unit 2e (~27 ka) combined with the molluscan and sedimentological records lead to the correlation of TG1 formation with GIS 3 (Fig. 12).

5.4.2. Sharp increase in loess sedimentation during the Upper Pleniglacial (~27–20 ka)

The transition from TG1 to the Upper Pleniglacial loess of units 2 and 1 is abrupt and marked by a drastic increase in sedimentation rate (Fig. 9) and a rapid decrease in mollusc abundance, diversity and hygrophilous, palustral and aquatic species (Fig. 7) due to a return to cold and arid conditions.

The last main sedimentation phase recorded at DV is composed of a thick sandy calcareous loess body. Fine sand content reaches 45% in unit 2 where 5–10 mm thick sand laminations are pervasive

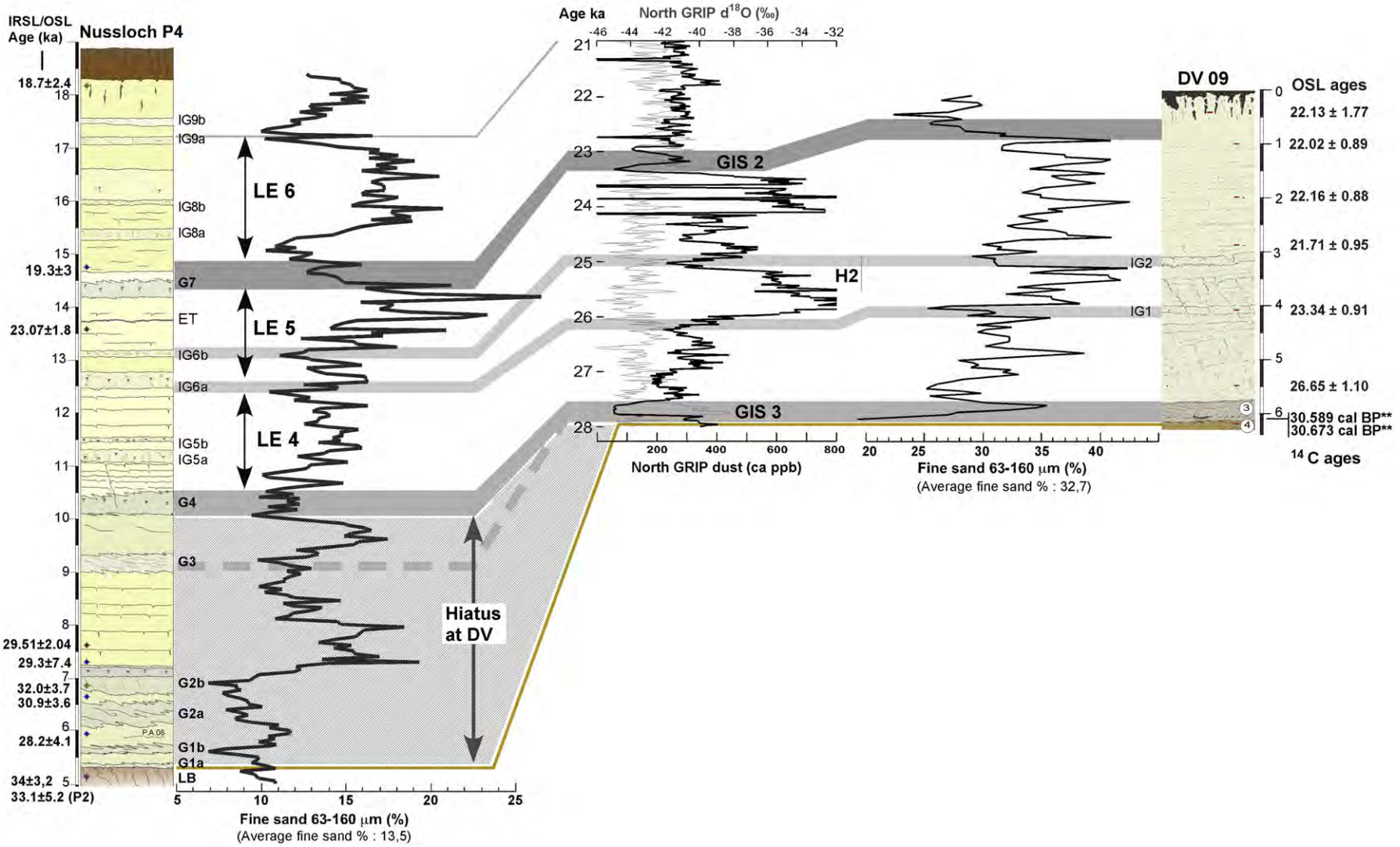

Fig. 12. Comparison between and the variation of fine sand fraction percentages at Nussloch and Dolní Věstonice with the NGRIP dust and $\delta^{18}O$ records (Nussloch data and LE events: according to Antoine et al., 2009a,b adapted, North GRIP $\delta^{18}O$, according to Svensson et al., 2008; GISPII dust according to Rasmussen et al., 2008).

and associated to a network of syngenetic frost-cracks (cryo-dessication). The high sand content implies an important local sediment source most likely the braided Dyje River valley system which geographically wraps around to the east, north and west the DV09 site and the topographic high of the Pavlov Mountain.

Unit 2 is also punctuated by two incipient tundra gleys IG1 and IG2 corresponding to sub-units 2d and 2b respectively identified in the field. In the analytical data set these incipient tundra gley layers are best identified by the shift towards more negative $\delta^{13}C$ values with respect to the underlying and overlying loess (Fig. 6) and the appearance of humidity-seeking taxa (*Arianta arbustorum* and *Succinea* species in IG1; *A. arbustorum* and *Succinea* species in IG2) and the disappearance of steppic taxa *Pupilla loessica*, *Helicopsis striata*, *Chondrula tridens* and *Euomphalia strigella* present in the loess (Ložek in Klima et al., 1962).

The transition from unit 2 to loess of unit 1 is marked by an almost 10% drop in fine sand content (Fig. 5), a 5–10% increase in $CaCO_3$ (Fig. 6) and an absence of laminations. This shift in loess characteristics is a feature observed in other Upper Pleniglacial loess records in Belgium and Northern France where finely laminated Hesbayen loess and homogeneous Brabantian loess above are separated by the Nagelbeek tongue horizon (Haesaerts et al., 1981). Half a metre below the boundary between unit 2 and 1, at 1.5 m depth, a net impoverishment of the malacofauna with only a low abundance of loess ubiquitous taxa (*Pupilla* sp., *Succinea* sp., *Helicacea* sp.) are observed. Similar changes in mollusc assemblage accompanied by a decrease in sediment grain size is also observed at the top of the Nussloch loess sequence (Moine et al., 2008) marking a global shift to drier conditions at the end of the Upper Pleniglacial starting at ~22 ka.

The soil at the top of the profile is a reworked humic topsoil including bricks fragments indicating that the top of the upper loess unit 1 has experienced erosion likely due to human impact since the Neolithic. The relatively old OSL age obtained ~0.4 m below the surface (BT 766: 22.17 ± 1.77 ka) supports the hypothesis that the youngest loess (~20–17 ka) at DV09 has been eroded.

The Upper Pleniglacial loess of DV09 totalling 6 m in depth shows facies typical of other contemporaneous loess deposits from Western Europe where average thickness for this time period range from ~3 to 6 m (Antoine et al., 1999a, 2003a,b). The Grain Size Index shows a global coarsening trend from the base of unit 2e to the top of 2a followed by a sharp decrease in unit 1 (Fig. 5). Superimposed on this trend, variations in sand percentage highlight a periodical pattern of coarse loess events. These periodic pulses of coarser aeolian deposition are observed in Upper Pleniglacial loess of Nussloch in Germany (Antoine et al., 2003a,b, 2009a), and other deposits in Northern France (Antoine et al., 1999a,b, 2003b), and more recently in Ukraine (Rousseau et al., 2011). They can be used to cross-correlate on continental scale loess records. Sub-unit 2e through 2a are proposed to be contemporaneous with Nussloch Loess Events 5 and 4 deposited between ~27 and 23 ka, whereas unit 1 was deposited at the same time as Nussloch Loess Event 6 at around 21–20 ka (Fig. 12). Incipient gleys 1 and 2 along DV09 would therefore correspond to IG 6a and 6b at Nussloch respectively.

6. Conclusions

The Dolní Věstonice (DV) reference sequence was sampled continuously and at a high-resolution and underwent various analyses (pedo-stratigraphy, thin sections, grain size, magnetic susceptibility, molluscs, $CaCO_3$, TOC, Organic carbon $\delta^{13}C$) crossing disciplinary boundaries and complemented by new chronological data based on optically-stimulated luminescence (Fuchs et al., 2012) and AMS ^{14}C techniques. The study's main results and conclusions are the following:

1) The pedo-stratigraphy of the Last Interglacial–Glacial record is re-defined and underlines four main sub-sequences separated by erosional boundaries or hiatus and characterized by major facies changes. The four sub-sequences are coeval to the Early-glacial, Lower, Middle and Upper Pleniglacial chrono-climatic units of European loess sequences. Despite clearly more continental conditions in DV (conclusion # 5 below), homogeneity among pedo-sedimentary records across Europe during the last climatic cycle is confirmed and provides further evidence of the influence of North Atlantic atmospheric circulation across western and Central Europe.
2) The data set demonstrates that the DV basal humic soil complex (BHSC) exhibits an exceptionally well preserved budget of the response to climate and environmental changes between ~110 and 70 ka. The response is archived through 7 individual pedo-sedimentary cycles permitting a reliable correlation with Greenland reference records (especially interstadials GIS 25 to 19). The DV BHSC can thus be considered as a new reference for the Weichselian Early-glacial in Europe. Within this soil complex, each individual interstadial event is characterized by a soil horizon that is very well depicted by markedly higher value in clay, TOC, mass specific bulk magnetic susceptibility and more negative $\delta^{13}C$ values. In addition, 5 aeolian silt layers (marker silts, MS) are observed within the BHSC intercalated with humic soil horizons. The MS are interpreted as regional dust storms deposits, occurring in continental steppe environments and correlating with cold events GS 25 to 20 and C 24 to C 19 in ice core and marine sediment records respectively between 110 and ~70 ka.
3) New chronological data provides supporting evidence for long hiatuses associated with erosional periods between the sub-sequences and most notably between ~35 and 25 ka at the boundary between the Middle brown soil complex and the Upper Pleniglacial loess (Fig. 12). Because of theses hiatuses and also the contrasting sedimentation rates correlations with global paleoclimate records is done on the Basal humic soil complex, the Lower Pleniglacial loess and the Upper Pleniglacial loess separately. Both OSL and radiocarbon ages show that the archeological layer transected in DV09 profile corresponds to younger periods of the Gravettian occupation in the area (~31 ka).
4) Grain size results confirm the GSI coarsening trend through both Lower and Upper Pleniglacial loess, the periodic coarse grain Loess Events associated with major storm events and the abrupt shift from laminated sandy loess to homogeneous loess at ~22 ka as previously reported elsewhere in Western and Central Europe.
5) The comparison with Western European sequences demonstrates that during the Early-glacial, climatic conditions in Moravia were markedly dryer than in Western Europe (chernozem soils, aeolian silt, and absence of hydromorphic features and of ice-lensing structures). However, during the Last Interglacial, oceanic temperate climatic conditions prevailed in both Moravia and Western Europe with the development of the similar brown leached soils (luvisols).

Acknowledgements

Research funding is provided through ANR-08-BLAN-0227 grant to DDR (PI) and PA, CH and FL (Co-PIs). This is contribution number 7654 of LDEO, 5050 of LSCE and 3352 of IPGP. The authors would like to express their sincere acknowledgements to the

Czech authorities for providing us the authorization to investigate the Dolní Věstonice loess sequence.

The authors thank Pr. D. Faust and the anonymous reviewer for their constructive and fair comments on the manuscript.

Appendix A. Supplementary data

Supplementary data related to this article can be found at http://dx.doi.org/10.1016/j.quascirev.2013.01.014.

References

Absolon, K., 1938a. Die Erforschung der diluvialen Mammutjägerstation von Unterwisternitz an den Pollauer Bergen bei Mähren. Arbeitsgericht über das erste Jahr 1924. Studien aus dem Gebiete der allgemeinen Karstforschung der wissenschaftlichen Höhlenkunde, der Eiszeitforschung und den Nachbargebieten. C, Palaeoethnologische Series 7 (5), 1–52.

Absolon, K., 1938b. Die Erforschung der diluvialen Mammutjägerstation von Unterwisternitz an den Pollauer Bergen bei Mähren. Arbeitsgericht über das zweite Jahr 1925. Brünn. Studien aus dem Gebiete der allgemeinen Karstforschung der wissenschaftlichen Höhlenkunde, der Eiszeitforschung und den Nachbargebieten. C, Palaeoethnologische Series 9 (6), 1–101.

Absolon, K., Žapletal, K., Skutil, J., Stehlik, A., 1933. Bericht der cechoslowakischen Subkommission der "The international commission for the study of the fossil man" bei den internationalen geologischen Kongressen. Studien aus dem Gebiete der allgemeinen Karstforschung der wissenschaftlichen Höhlenkunde, der Eiszeitforschung und den Nachbargebieten. C, Palaeoethnologische Series 1 (3), 1–7.

Alfaro, S.C., Gomes, L., 2001. Modeling mineral aerosol production by wind erosion: emission intensities and aerosol size distributions in source areas. Journal of Geophysical Research 106, 18075–18084.

Andersen, K.K., Svensson, A., Johnsen, S.J., Rasmussen, S.O., Bigler, M., Röthlisberger, R., Ruth, R., Siggaard-Andersen, M.-L., Steffensen, J.-P., Dahl-Jensen, D., Vinther, B.M., Clausen, H.B., 2006. The Greenland Ice core chronology 2005, 15–42 ka. Part 1: constructing the time scale. Quaternary Science Reviews 25, 3246–3257.

Antoine, P., Rousseau, D.D., Lautridou, J.P., Hatté, C., 1999a. Last Interglacial–Glacial climatic cycle in loess-palaeosol successions of north-western France. Boreas 28, 551–563.

Antoine, P., Bonifay, E., Conchon, O., Legigan, P., Lautridou, J.-P., Macaire, J.-J., Mandier, P., Monnier, J.-L., Morzadec, M.-T., Revel, J.-C., Sommé, J., Tastet, J.-P., 1999b. Extension des loess et sables éoliens à 18±2 ka en France. In: INQUA, ANDRA (Eds.), La France pendant les deux derniers extrêmes climatiques, variabilité naturelle des environnements. cartes au 1/1 000 000 et notice explicative, pp. 22–26.

Antoine, P., Rousseau, D.D., Zöller, L., Lang, A., Munaut, A.V., Hatté, C., Fontugne, M., 2001. High resolution record of the Last Interglacial–Glacial cycle in the Nussloch loess-palaeosol sequences, Upper Rhine Area Germany. Quaternary International 76-77, 211–229.

Antoine, P., Rousseau, Hatté, C., Zöller, L., Lang, A., Fontugne, M., Moine, O., 2002. Événements éoliens rapides en contexte loessique: l'exemple de la séquence du Pléniglaciaire supérieur weichselien de Nussloch (Vallée du Rhin-Allemagne). Quaternaire 13, 3–4. 199–208.

Antoine, P., Bahain, J.-J., Debenham, N., Frechen, M., Gauthier, A., Hatté, C., Limondin-Lozouet, N., Locht, J.-L., Raymond, P., Rousseau, D.-D., 2003a. Nouvelles données sur le Pléistocène du Nord du Bassin Parisien: les séquences loessiques de Villiers-Adam (Val d'Oise, France). Quaternaire 14, 219–235.

Antoine, P., Catt, J., Lautridou, J.P., Sommé, J., 2003b. The loess and coversands of northern France and Southern England. Journal of Quaternary Sciences 18, 309–318.

Antoine, P., Rousseau, D.D., Moine, O., Kunesch, S., Hatté, C., Lang, A., Zöller, L., 2009a. Evidence of rapid and cyclic eolian deposition during the Last Glacial in European loess series (Loess events): the high-resolution records from Nussloch (Germany). Quaternary Science Reviews 28, 2955–2973.

Antoine, P., Rousseau, D.D., Fuchs, M., Hatté, C., Marcovic, S.B., Jovanovic, M., Gaudenyi, T., Moine, O., Rossignol, J., 2009b. High resolution record of the last climatic cycle in the southern Carpathian basin at Surduk (Vojvodina, Serbia). Quaternary International 198, 19–36.

Auffret, J.P., Horn, R., Larsonneur, C., Curry, D., Smith, A., 1982. La Manche orientale, carte des paléovallées et des bancs sableux. Bureau de Recherches Géologiques et Minières éditions 1982.

Bábek, O., Chlachula, J., Grygar, T.M., 2011. Non-magnetic indicators of pedogenesis related to loess magnetic enhancement and depletion: examples from the Czech Republic and southern Siberia. Quaternary Science Reviews, 1–13.

Beresford-Jones, D., Taylor, S., Paine, C., Pryor, A., Svoboda, J., Jones, M., 2011. Rapid climate change in the Upper Palaeolithic: the record of charcoal conifer rings from the Gravettian site of Dolní Věstonice, Czech Republic. Quaternary Science Reviews 30, 1948–1964.

Boch, R., Cheng, H., Spötl, R., Edwards, L., Wang, X., Häuselmann, Ph, 2011. NALPS: a precisely dated European climate record 120–60 ka. Climate of the Past 7, 1247–1259.

Bohmers, A., 1941. Die Ausgrabungen bei Unter-Wisternitz. Forschungen und Fortschritte 17 (3), 21–22.

Buurman, P., Pape, T., Reijneveld, J.A., De Jong, F., Van Gelder, E., 2001. Laser-diffraction and pipette-method grain sizing of Dutch sediments: correlations for fine fractions of marine, fluvial, and loess samples. Netherlands Journal of Geosciences 80 (2), 49–57.

Catt, J.A., 1985. Soil particle size distribution and mineralogy as indicators of pedogenic and geomorphic history: examples from the loessial soils of England Wales. In: Richard, K.S., Arnet, R.R., Ellis, S. (Eds.), Geomorphology and Soils. G. allen and Unwin, London, pp. 202–218.

Catt, J.A., 1988. Soils and Quaternary stratigraphy in the United Kingdom. In: Boardman, J.W. (Ed.), Quaternary Geology for Scientists and Engineers. Ellis Horwood, Chichester, pp. 161–178.

Chapman, M.R., Shackleton, N.J., 1999. Global ice-volume fluctuations, North Atlantic ice-rafting events, and deep-ocean circulation changes between 130 and 70 ka. Geology 27, 795–798.

Cilek, V., 2001. The loess deposits of the Boheian Massif: silt provenance, palaeometeorology and loessification processes. Quaternary International 76-77, 123–128.

Damblon, Haesaerts, 1997. Radiocarbon chronology of representative Upper palaeolithic sites in the Central European Plain: a contribution to the SC-004 project. Préhistoire Européenne 11, 255–276.

Demek, J., Kukla, J., 1969. Periglazialzone Löss und Paläolithikum der Tschechoslowakei. Czechoslovak Academy of Science, Institut of Geography, Brno, Czechoslovakia, Brno. 157.

Eckmeier, E., Gerlach, R., Gehrt, E., Schmidt, M.W.I., 2007. Pedogenesis of Chernozems in Central Europe – a review. Geoderma 139, 288–299.

Ehlers, J., Gibbard, P., Hughes, P.D. (Eds.), 2011. Quaternary Glaciations – Extent and Chronology: a Closer Look. Developments in Quaternary Science, vol. 15. Elsevier, Amsterdam, p. 1126.

Forster, T., Heller, F., Evans, M.E., Havlicek, P., 1996. Loess in the Czech Republic: magnetic properties and paleoclimate. Studia Geophysica Et Geodaetica 40, 243–261.

Frechen, M., 1999. Upper Pleistocene loess stratigraphy in southern Germany. Quaternary Geochronology 18, 243–269.

Frechen, M., Schirmer, W., 2011. Luminescence chronology of the Schwalenberg II loess in the middle Rhine Valley. Eiszeitalter und Gegenwart 60-1, 78–89.

Frechen, M., Zander, A., Cilek, V., Ložek, V., 1999. Loess chronology of the Last Interglacial/Glacial cycle in Bohemia and Moravia, Czech Republic. Quaternary Science Reviews 18, 1467–1493.

Frechen, M., van Vliet-Lanoë, B., van den Haute, P., 2001. The Upper Pleistocene loess record at Harmignies/Belgium- high resolution terrestrial archive of climate forcing. Paleogeography, Paleoclimatology, Paleoecology 173, 175–195.

Frechen, M., Oches, E.A., Kohfeld, K.E., 2003. Loess in Europe-mass accumulation rates during the Last Glacial Period. Quaternary Science Reviews 22, 1835–1857.

Fuchs, M., Rousseau, D.D., Antoine, P., Hatté, C., Gauthier, C., 2007. Chronology of the Last Climatic Cycle (Upper Pleistocene) of the Surduk loess sequence, Vojvodina, Serbia. Boreas 10, 1–8.

Fuchs, M., Kreutzer, S., Rousseau, D.D., Antoine, P., Hatté, C., Lagroix, F., Moine, O., Gauthier, C., Svoboda, J., Lisá, L., 2012. The loess sequence of Dolní Věstonice (Czech Republic): a new OSL based chronology of the Last Climatic Cycle. Boreas. http://dx.doi.org/10.1111/j.1502–3885.2012.00299.x.

Gauthier, C., Hatté, C., 2008. Effects of handling, storage, and chemical treatments on delta C-13 values of terrestrial fossil organic matter. Geophysics, Geochemistry and Geosystem 9, Q08011. http://dx.doi.org/10.1029/2008GC001967.

Gerasimenko, N., 2006. Upper Pleistocene loess-palaeosol and vegetational successions in the Middle Dnieper Area, Ukraine. Quaternary International 149, 55–66.

Gerasimenko, N., Rousseau, D.-D., 2008. Stratigraphy and paleoenvironments of the last Pleniglacial in the Kyiv loess region (Ukraine). Quaternaire 19, 293–307.

Gerasimova, M., 2003. Higher levels of description - approaches to the micromorphological characterisation of Russian soils. Catena 54, 319–337.

Gerasimova, M.I., Gubin, S.V., Shoba, S.A., 1996. In: Miedema, R.Ž. (Ed.), Soils of Russia and Adjacent Countries: Geography and Micromorphology. Moscow-Wageningen, p. 204.

Grini, A., Zender, C., 2004. Roles of saltation, sandblasting, and wind speed variability on mineral dust aerosol size distribution during the Puerto Rican Dust Experiment (PRIDE). Journal of Geophysical Research 109, D07202. http://dx.doi.org/10.1029/02003JD004233.

GRIP Members, 1993. Climate instability during the last interglacial period recorded in the GRIP ice-core. Nature 364, 203–207.

Guihou, A., Pichat, S., Nave, S., Govin, A., Labeyrie, L., Michel, E., Waelbroeck, C., 2011. A late slowdown of the Atlantic Meridional overturning circulation during the Last Glacial inception: new constraints from sedimentary (231Pa/230Th). Earth and Planetary Science Letters 289, 520–529.

Guthrie, D., 2001. Origin and cause of the Mammoth steppe: a story of cloud cover, wolly mammal tooth pits, buckles and inside-out Beringia. Quaternary Science Reviews 20, 549–574.

Haase, D., Fink, J., Haase, G., Ruske, R., Pécsi, M., Richter, H., Altermann, M., Jäger, K.-D., 2007. Loess in Europe – its spatial distribution based on a European loess map, scale 1:2,500,000. Quaternary Science Reviews 26, 1301–1312.

Haesaerts, P., Mestdagh, H., 2000. Pedosedimentary evolution of the last interglacial and early glacial sequence in the European loess belt from Belgium to central Russia. Geologie en Mijnbouw 79, 313–324.

Haesaerts, P., Juvigné, E., Kuyl, O., Mücher, H., Roebroeks, W., 1981. Compte rendu de l'excursion du 13 Juin 1981, en Hesbaye et au Limbourg Néerlandais, consacrée à la chronostratigraphie des loess du Pléistocène supérieur. Annales de la Société Géologique de Belgique 104, 223–240.
Haesaerts, P., Damblon, F., Bachner, M., Trnka, G., 1996. Revised Stratigraphy and Chronology of the Willendorf II Sequence, Lower Austria, vol. 80. Archaeologia Austriaca, Wien. 25–42.
Haesaerts, P., Mestdagh, H., Bosquet, D., 1999. The sequence of Remicourt (Hesbaye-Belgium): new insights on the pedo and chronostratigraphy of the Rocourt Soil. Geologica Belgica 2 (3/43), 5–27.
Haesaerts, P., Borziak, I., Chirica, V., Damblon, F., Koulakovska, L., Van der Plicht, J., 2003. The East-Carpathian loess record: a reference for the Middle and Late Pleniglacial stratigraphy in Central Europe. Quaternaire 14 (3), 163–188.
Hatté, C., Fontugne, M., Rousseau, D.D., Antoine, P., Zöller, L., Tisnéra-Laborde, N., Bentaleb, I., 1998. ^{13}C Variations of loess organic matter as a record of the vegetation response to climatic changes during the Weichselian. Geology 26 (7), 583–586.
Hatté, C., Antoine, P., Fontugne, M., Rousseau, D.D., Tisnéra-Laborde, N., Zöller, L., 1999. New chronology and organic matter $\delta^{13}C$ paleoclimatic significance of Nussloch loess sequence (Rhine Valley, Germany). Quaternary International 62, 85–91.
Hatté, C., Antoine, P., Fontugne, M., Lang, A., Rousseau, D.D., Zöller, L., 2001a. $\delta^{13}C$ of loess organic matter as a potential proxy for paleoprecipitation. Quaternary Research 55, 33–38.
Hatté, C., Pessenda, L.C., Lang, A., Paterne, M., 2001b. Development of accurate and reliable ^{14}C chronologies for loess deposits: application to the loess sequence of Nussloch (Rhine Valley, Germany). Radiocarbon 43 (2B), 611–618.
Hatté, C., Morvan, J., Noury, C., Paterne, M., 2001c. Is classical acid-alkali-acid treatment responsible for contamination? An alternative proposition. Radiocarbon 43 (2A), 177–182.
Horvath, E., 2001. Marker horizons in the loesses of the Carpathian Basin. Quaternary International 76-77, 57–163.
Juvigné, E., Haesaerts, P., Metsdagh, H., Balescu, S., 1996. Révision du stratotype loessique de Kesselt (Limbourg, Belgique). Compte Rendu de l'Académie des Sciences, Paris, série IIa 323, 801–807.
Klein Tank, A.M.G., Wijngaard, J.B., Können, G.P., Böhm, R., Demarée, G., Gocheva, A., Mileta, M., Pashiardis, S., Hejkrlik, L., Kern-Hansen, C., Heino, R., Bessemoulin, P., Müller-Westermeier, G., Tzanakou, M., Szalai, S., Pálsdóttir, T., Fitzgerald, D., Rubin, S., Capaldo, M., Maugeri, M., Leitass, A., Bukantis, A., Aberfeld, R., van Engelen, A.F.V., Forland, E., Mietus, M., Coelho, F., Mares, C., Razuvaev, V., Nieplova, E., Cegnar, T., Antonio López, J., Dahlström, B., Moberg, A., Kirchhofer, W., Ceylan, A., Pachaliuk, O., Alexander, L.V., Petrovic, P., 2002. Daily dataset of 20th-century surface air temperature and precipitation series for the European climate assessment. International Journal of Climatology 22 (12), 1441–1453.
Klima, B., Kukla, G., Ložek, V., De Vries, H., 1962. Stratigraphie des Pleistozäns und Alter des palaeolitischen Rastplatzes in der Ziegelei von Dolní Věstonice (Unter-Wisternitz). Anthropozoikum 11, 93–145.
Konert, M., Vandenberghe, J., 1997. Comparison of laser grain size analysis with pipette and sieve analysis: a solution for the underestimation of the clay fraction. Sedimentology 44, 523–535.
Kovanda, J., 1979. The snail *Vertigo heldi* (Clessin, 1877) from the base of the youngest loesses of Dolní Věstonice (southern Moravia). Vestník Ústredního ústavu geologického 54 (2), 119–122.
Kovanda, J., 1991. Molluscs from the section with the skeleton of Upper Palaeolithic man at Dolní Věstonice. Etudes et Recherches Archéologiques de l'Université de Liège 54, 89–96.
Kreutzer, S., Fuchs, M., Meszner, S., Faust, D., 2012. OSL chronostratigraphy of a loess-palaeosol sequence in Saxony/Germany using quartz of different grain sizes. Quaternary Geochronology 359. http://dx.doi.org/10.1016/j.quageo.2012.01.004.
Kukla, G., 1961. Quaternary sedimentation cycle. In: Survey of the Czechoslovak Quaternary. Czwartorzed Europy srodkovej wschodniej. INQUA 6th International Congress, vol. 34. Inst. Geol Prace, Warszawa, pp. 145–154.
Kukla, G., 1975. Loess stratigraphy of Central Europe. In: Butzer, K.W., Isaac, G.L. (Eds.), After the Australopithecines. Mouton Publishers, The Hague, pp. 99–188.
Kukla, G.J., 1977. Pleistocene land-sea correlations I. Europe. Earth Science Review 13, 307–374.
Lais, R., 1954. Über den Löß von Unterwisternitz (Mähren). Palaeohistoria 2, 135–170.
Lang, A., Hatté, C., Rousseau, D.-D., Antoine, P., Fontugne, M., Zöller, L., Hambach, U., 2003. High-resolution chronologies for loess: comparing AMS ^{14}C and optical dating results. Quaternary Science Reviews, Quaternary Geochonology 22, 953–959.
Lautridou, J.-P., 1987. Le cycle périglaciaire pléistocène en Europe du Nord-Ouest et plus particulièrement en Normandie. Thèse Lettres, Univ. Caen, 1985, vol. 2, 908 pp.
Lautridou, J.-P., Sommé, J., Heim, J., Puisségur, J.J., Rousseau, D.D., 1985. La stratigraphie des læss et formations fluviatiles d'Achenheim (Alsace): nouvelles données bioclimatiques et corrélations avec les séquences pléistocènes de la France du Nord-Ouest. Bulletin de l'Association Française pour l'Etude du Quaternaire 22, 125–132.
Lisa, L., Uher, P., 2006. Provenance of würmian loess and loess-like sediments of Moravia and Silesia (Czech Republic): a study of zircon typology and cathodoluminescence. Geologica Carpathica 57-5, 397–403.
Lisiecki, L.E., Raymo, M.E., 2005. A Pliocene-Pleistocene stack of 57 globally distributed benthic $\delta^{18}O$ records. Paleoceanography 20, PA 1003.
Ložek, V., 1953. Pleistocénní mekkýši z gravettského sídliště u Dolních Vestonic. Monumenta Archeologica 2, 45–51.
Ložek, V., 1964. Quartärmollusken der Tschechoslowakei. Rozpravy Ústredního ústuvu geologického 31, 1–374.
Maher, B., 2011. The magnetic properties of Quaternary aeolian dusts and sediments, and their palaeoclimatic significance. Aeolian Research 3, 87–144.
Maher, B.A., Taylor, R.M., 1988. Formation of ultrafine-grained magnetite in soils. Nature 336, 368–370.
Marković, S.B., Bokhorst, M., Vandenberghe, J., Oches, E.A., Zöller, L., McCoy, W.D., Gaudenyi, T., Jovanović, M., Hambach, U., Machalett, B., 2008. Late Pleistocene loess-paleosol sequences in the Vojvodina region, North Serbia. Journal of Quaternary Science 23, 73–84.
Martrat, B., Grimalt, J.O., Shackleton, N.J., de Abreu, L., Hutterli, M.A., Stocker, T.F., 2007. Four climate cycles of recurring deep and surface water destabilizations on the Iberian Margin. Science 317, 502–507.
Meijs, E.P.M., 2002. Loess stratigraphy in Dutch and Belgian Limburg. Eiszeitalter und Gegenwart 51, 114–130.
Meszner, S., Fuchs, M., Faust, D., 2011. Loess-paleosol-sequences from the loess area of saxony (Germany). E & G, Quaternary Science Journal 60, 47–65.
Moine, O., Rousseau, D.D., Antoine, P., Hatté, C., 2002. Mise en évidence d'événements climatiques rapides par les faunes de mollusques terrestres des loess weichseliens de Nussloch (Allemagne). Quaternaire 13 (3–4), 209–218.
Moine, O., Rousseau, D.-D., Antoine, P., 2008. The impact of Dansgaard-Oeschger cycles on the loessic environment and malacofauna of Nussloch (Germany) during the Upper Weichselian. Quaternary Research 70 (1), 91–104.
Moine, O., Antoine, P., Deschodt, L., Sellier, N., 2011. Enregistrements malacologiques à haute résolution dans les loess et les gleys de toundra du pléniglaciaire weichselien supérieur: premiers exemples du nord de la France. Quaternaire 22-4, 307–325.
Müller, U.C., Pross, J., Bibus, E., 2003. Vegetation response to rapid climate change in Central Europe during the past 140,000 yr based on evidence from the Füramoos pollen record. Quaternary Research 59, 235–245.
Musson, F., Wintle, A.G., 1994. Luminescence dating of the loess profile at Dolní Věstonice, Czech Republic. Quaternary Geochronology 13, 411–416.
NGRIP Members, 2004. High resolution climate record of the northern hemisphere reaching into the Last Glacial interglacial period. Nature 431, 147–151.
Novothny, Á., Frechen, M., Horvath, E., Wacha, L., Rolf, C., 2011. Investigating the penultimate and last glacial cycles of the Sütto loess section (Hungary) using luminescence dating, high-resolution grain size, and magnetic susceptibility data. Quaternary International 234 (1–2), 75–85.
Nugteren, G., Vandenberghe, J., van Huissteden, K., Zhisheng, A., 2004. A Quaternary climate record based on grain size analysis from the Luochuan loess section on the Central Loess Plateau, China. Global and Planetary Change 41, 167–183.
Oches, E.A., Banerjee, S.K., 1996. Rock-magnetic proxies of climate change from loess – paleosol sediments of the Czech Republic. Studia Geophysica Et Geodaetica 40, 287–300.
Oches, E.A., McCoy, W.D., 1995. Aminostratigraphic evaluation of conflicting age estimates for the « Young Loess' of Hungary. Quaternary Research 44, 160–170.
Pendea, I.F., Gray, J.T., Ghaleb, B., Tantau, I., Badarau, A.S., Nicorici, C., 2009. Episodic build-up of alluvial fan deposits during the Weichselian Pleniglacial in the western Transylvanian Basin, Romania and their paleoenvironmental significance. Quaternary International 198, 98–112.
Petrbok, J., 1951a. Plistocenní měkkýsi vodních sedimentů paleolitocké stanice Dolních Věstonic (Jihomoravsky Kras). Československý Kras 4 (5), 121.
Petrbok, J., 1951b. Plistocenní měkkýsi aurignacackého sídliště Dolních Věstonic. Československý Kras 4 (9), 256–257.
Ramaswany, V., Rao, P.S., 2006. Grain size analysis of sediments from the northern Andaman sea: comparison of laser diffraction and sieve-pipette techniques. Journal of Coastal Research 22 (4), 1000–1009.
Rasmussen, S.O., Seierstad, I.K., Andersen, K.K., Bigler, M., Dahl-Jensen, D., Johnsen, S.J., 2008. Synchronization of the NGRIP, GRIP, and GISP2 ice cores across MIS 2 and palaeoclimatic implications. Quaternary Science Reviews 27, 18–28.
Reimer, P.J., Baillie, M.G.L., Bard, E., Bayliss, A., Beck, J.W., Blackwell, P.G., Bronk Ramsey, C., Buck, C.E., Burr, G.S., Edwards, R.L., Friedrich, M., Grootes, P.M., Guilderson, T.P., Hajdas, I., Heaton, T.J., Hogg, A.G., Hughen, K.A., Kaiser, K.F., Kromer, B., McCormac, F.G., Manning, S.W., Reimer, R.W., Richards, D.A., Southon, J.R., Talamo, S., Turney, C.S.M., van der Plicht, J., Weyhenmeyer, C.E., 2009. IntCal09 and Marine09 radiocarbon age calibration curves, 0–50,000 years cal BP. Radiocarbon 51 (4), 1111–1150.
Richter, D., Tostevin, G., Skrdla, P., Davies, W., 2009. New radiometric ages for the Early Upper Palaeolithic type locality of Brno-Bohunice (Czech Republic): comparison of OSL, IRSL, TL and 14C dating results. Journal of Archaeological Science 36, 708–720.
Rousseau, D.D., Kukla, G., Zöller, L., Hradilova, J., 1998a. Early Weichselian dust storm layer at Achenheim in Alsace, France. Boreas 27 (3), 200–207.
Rousseau, D.D., Zöller, L., Valet, J.P., 1998b. Late Pleistocene climatic variations at Achenheim, France, based on a magnetic susceptibility and TL chronology of loess. Quaternary Research 49, 255–263.
Rousseau, D.D., Gerasimenko, N., Matviischina, Z., Kukla, G., 2001. Late Pleistocene environments of the central Ukraine. Quaternary Research 56 (3), 349–356.
Rousseau, D.-D., Antoine, P., Hatté, C., Lang, A., Zöller, L., Fontugne, M., Ben Othman, D., Luck, J.-M., Moine, O., Labonne, M., Bentaleb, I., Jolly, D., 2002. Abrupt millennial climatic changes from Nussloch (Germany) Upper

Weichselian eolian records during the Last Glaciation. Quaternary Science Reviews 21, 1577–1582.
Rousseau, D.-D., Sima, A., Antoine, P., Hatté, C., Lang, A., Zöller, L., 2007. Link between European and North-Atlantic abrupt climate changes over the last glaciation. Geophysical Research Letters 34, L22713. http://dx.doi.org/10.1029/2007/GL031716.
Rousseau, D.-D., Antoine, P., Gerazimenko, N., Sima, A., Hatté, C., Moine, O., Zöller, L., 2011. North Atlantic abrupt climatic events of the last glacial period recorded in Ukrainian loess deposits. Climate of the Past 7, 221–234. http://dx.doi.org/10.5194/cp-7-221-2011.
Sánchez Goñi, M.F., Cacho, I., Turon, J.-L., Guiot, J., Sierro, F.J., Peypouquet, J.-P., Grimalt, J.O., Shackleton, N.J., 2002. Synchronicity between marine and terrestrial responses to millennial scale climatic variability during the last glacial period in the Mediterranean region. Climate Dynamics 19, 95–105.
Sánchez Goñi, M.F., 2006. Interactions végétation-climat au cours des derniers 425.000 ans en Europe occidentale. Le message du pollen des archives marines. Quaternaire 17-1, 3–25.
Schirmer, W., 2000. O-stages 2-5 in the Rhein loess, ice cores and deep-sea cores. Quaternary International 63-64, 129.
Schmidt, M.V.I., Skjemstad, J.O., Gehrt, E., Kögel-Knabner, I., 1999. Charred organic carbon in German chernozemic soils. European Journal of Soil Science 50, 351–365.
Shackleton, N.J., Hall, M.A., Vincent, E., 2000. Phase relationships between millennial-scale events 64,000–24,000 years ago. Paleoceanography 15, 565–569.
Shackleton, N.J., Chapman, M., Sánchez Goñi, M.F., Pailler, D., Lancelot, Y., 2002. The Classic Marine Isotope Substage 5e. Quaternary Research 58, 14–16.
Shackleton, N.J., Sánchez Goñi, M.F., Pailler, D., Lancelot, Y., 2003. Marine Isotope Substage 5e and the Eemian Interglacial. Global and Planetary Change 36, 151–155.
Shackleton, N.J., Fairbanks, R.G., Chiu, T.-C., Parrenin, F., 2004. Absolute calibration of the Greenland time scale: implications for Antarctic time scales and for $\delta^{14}C$. Quaternary Science Reviews 23, 1513–1522.
Shi, C., Zhu, R., Glass, B.P., Liu, Q., Zema, A., Suchy, V., 2003. Climate variations since the last interglacial recorded in Czech loess. Geophysical Research Letters 30 (11), 161–164.
Sima, A., Rousseau, D.-D., Kageyama, M., Ramstein, G., Schulz, M., Balkansky, Y., Antoine, P., Dulac, F., Hatté, C., 2009. North-Atlantic millennial-timescale variability imprint on Western European loess deposits: a modeling study. Quaternary Science Reviews 28, 2851–2866.
Sirocko, F., Seelos, K., Schaber, K., Rein, B., Dreher, F., Diehl, M., Lehne, R., Jäger, K., Krbetschek, M., Degring, D., 2005. A late Eemian aridity pulse in Central Europe during the last glacial inception. Nature 436, 833–836.
Smalley, I., O'Hara-Dhanda, K., Winta, J., Machalett, B., Jary, Z., Ian Jeffersone, I., 2009. Rivers and loess: the significance of long river transportation in the complex event-sequence approach to loess deposit formation. Quaternary International 198, 7–18.
Sommé, J., Paepe, R., Lautridou, J.P., 1980. Principes, méthodes et système de la stratigraphie du Quaternaire dans le Nord-Ouest de la France et la Belgique. In: Problèmes de stratigraphie quaternaire en France et dans les pays limitrophes. Supplément au Bulletin de l'Association Française pour l'Etude du Quaternaire NS-1, pp. 148–162.
Sommé, J., Lautridou, J.P., Heim, J., Maucorps, J., Puisségur, J.J., Rousseau, D.D., Thévenin, A., Van Vliet-Lanoë, B., 1986. Le cycle climatique du Pléistocène supérieur dans les loess d'Alsace à Achenheim. Supplément au Bulletin de l'Association Française pour l'Etude du Quaternaire 23, 97–104.
Stevens, T., Markovic, S.B., Zech, M., Hambach, U., Sumegi, P., 2011. Dust deposition and climate in the Carpathian Basin over an independently dated last glacial-interglacial cycle. Quaternary Science Reviews 30, 662–681.
Svensson, A., Andersen, K.K., Bigler, M., Clausen, H.B., Dahl-Jensen, D., Davies, S.M., Johnsen, S.J., Muscheler, R., Parrenin, F., Rasmussen, S.O., Röthlisberger, R., Seierstad, I., Steffensen, J.P., Vinther, B.M., 2008. A 60 000 year Greenland stratigraphic ice core chronology. Climate of the Past 4, 47–57.
Svoboda, J., 1995. Environment and Upper Palaeolithic adaptations in Moravia. In: Ullrich, H. (Ed.), Man and the Environment in the Palaeolithic. Proceedings of the Symposium Neuwied (Germany), vol. 62. ERAUL, Liège, pp. 291–295.
Svoboda, J., 2001. Czech Republic: Projects of the Center for Palaeolithic and Paleoethnological Research (Institute of Archaeology, Academy of Sciences). In: Brno- Dolní Věstonice, vol. 97. ERAUL, Liège, pp. 73-88.
Svoboda, H., 1991. The pollen analysis of Dolní Věstonice II section No1. In: Svoboda, J. (Ed.), Dolní Věstonice II Western Slope, vol. 54. ERAUL, Liège.
Terhorst, B., Thiel, C., Peticzka, R., Sprafke, T., Frechen, M., Fladerer, F.A., Roetzel, R., Neugebauer-Maresch, C., 2011. Casting new light on the chronology of the loess/paleosol sequences in Lower Austria. Eiszeitalter und Gegenwart 60, 270–277.
Tisnérat-Laborde, N., Poupeau, J.-J., Tannau, J.-F., Paterne, M., 2001. Development of a semi-automated system for routine preparation of carbonate sample. Radiocarbon 43, 299–304.
Tissoux, H., Valladas, H., Voinchet, P., Reyss, J.L., Mercier, N., Falguères, C., Bahain, J.J., Zöller, L., Antoine, P., 2009. OSL and ESR studies of aeolian quartz sediments from the Upper Pleistocene loess sequence of Nussloch (Germany). Quaternary Geology. http://dx.doi.org/10.1016/j.quageo.2009.03.009. Special Issue LED, 2008.
Valoch, K., 1976. Die altsteinzeitliche Fundstelle in Brno-Bohunice. In: Studie Archeologickeho ustavu Ceskoslovenske Akademie ved v Brne, Brno, vol. 4.
Van der Maarel, E., 1980. On the interpretability of ordination diagrams. Vegetation 42 (1–3), 43–45.
Vandenberghe, J., Nugteren, G., 2001. Rapid climatic changes recorded in loess next term successions. Global and Planetary Change 28, 1–9.
Vandenberghe, J., Huijzer, B., Mücher, H., Laan, W., 1998. Short climatic oscillations in a western European loess sequence (Kesselt, Belgium). Journal of Quaternary Science 13, 471–485.
World reference base for soil resources (WRB), 1998. World Soil Resources Reports 84. Food and Agricultural Organization of the United Nations, Rome, 88 pp.
Zöller, L., Wagner, G., 1990. Thermoluminescence dating of loess-recent developments. Quaternary International 7/8, 119–128.
Zöller, L., Stremme, H.E., Wagner, G.A., 1988. Thermolumineszenz-Datierung an Löss-Paläoboden-Sequenzen von Nieder-, Mittle-und Obberhein. Chemical Geology: Isotope Geoscience Section 73, 39–62.
Zöller, L., Oches, E.A., McCoy, W.D., 1994. Towards a revised chronostratigraphy of loess in Austria with respect to key sections in the Czech Republic and in Hungary. Quaternary Geochronology 13, 465–472.